Remote Sensing by thermal emission

- Temperature Sounding
- SST from thermal IR ("split window")
- Humidity (profiles, upper tropospheric)
- Trace Gases (limb profiling)
- IR Clouds (AIRS, MODIS, etc)
- Microwave total column water vapor, cloud water, surface wind speed

Reference:

Chapter 7 of "Remote Sensing of the lower atmosphere"

Reminder: The fundamental equation

$$I_\lambda(0,\mu) = \underbrace{I_\lambda(\tau^*,\mu)\mathrm{e}^{-\tau^*/\mu}}_{\text{Surface term}} + \underbrace{\int_0^{\tau^*} B_\lambda(\tau)\,\mathrm{e}^{-\tau/\mu}\,\frac{d\tau}{\mu}}_{\text{Atmospheric emission}}$$

The emission spectrum

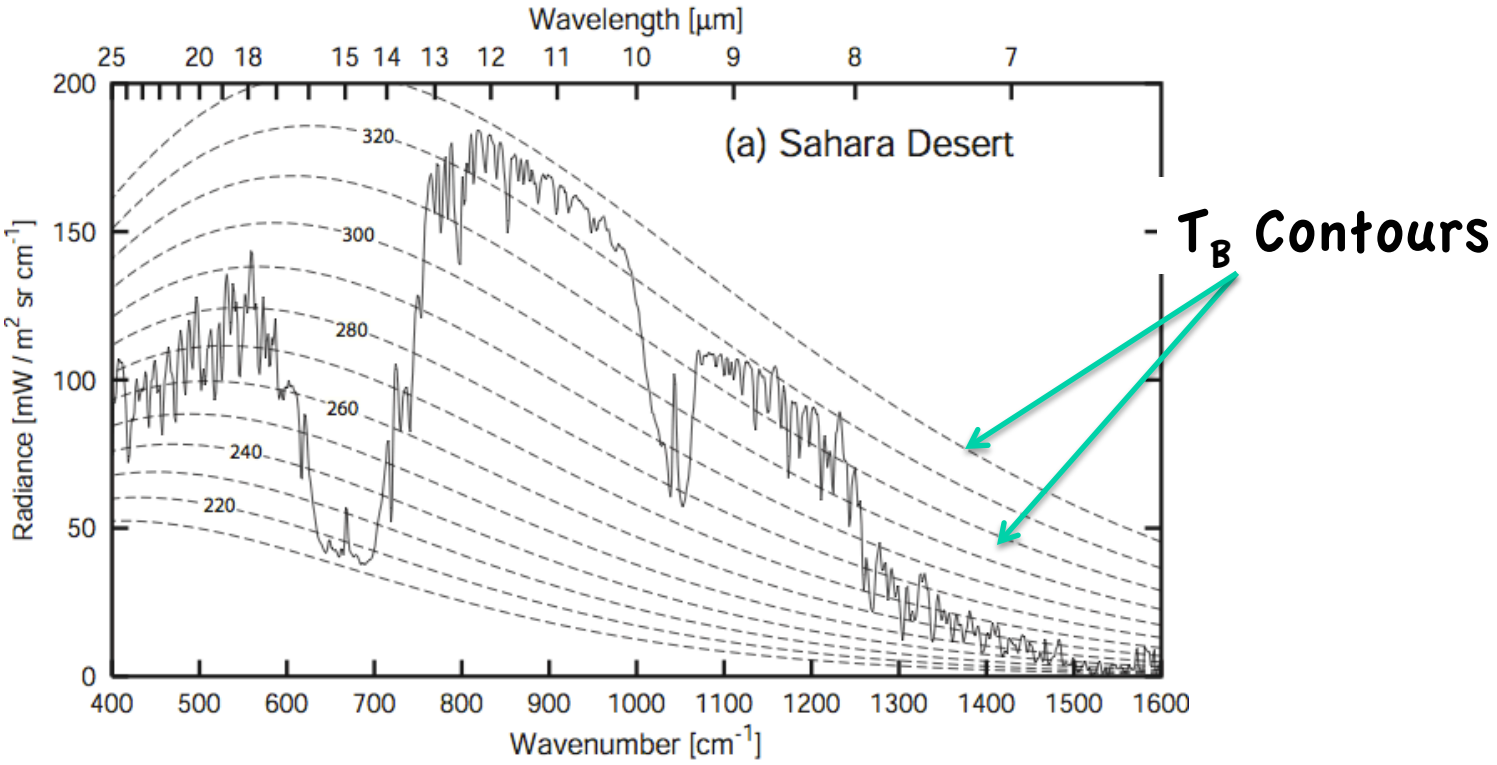

Information about the atmosphere and surface are encoded in these emission spectra

Extract this information requires in principle just using the (simple) RT equation with emission.

The emission spectrum

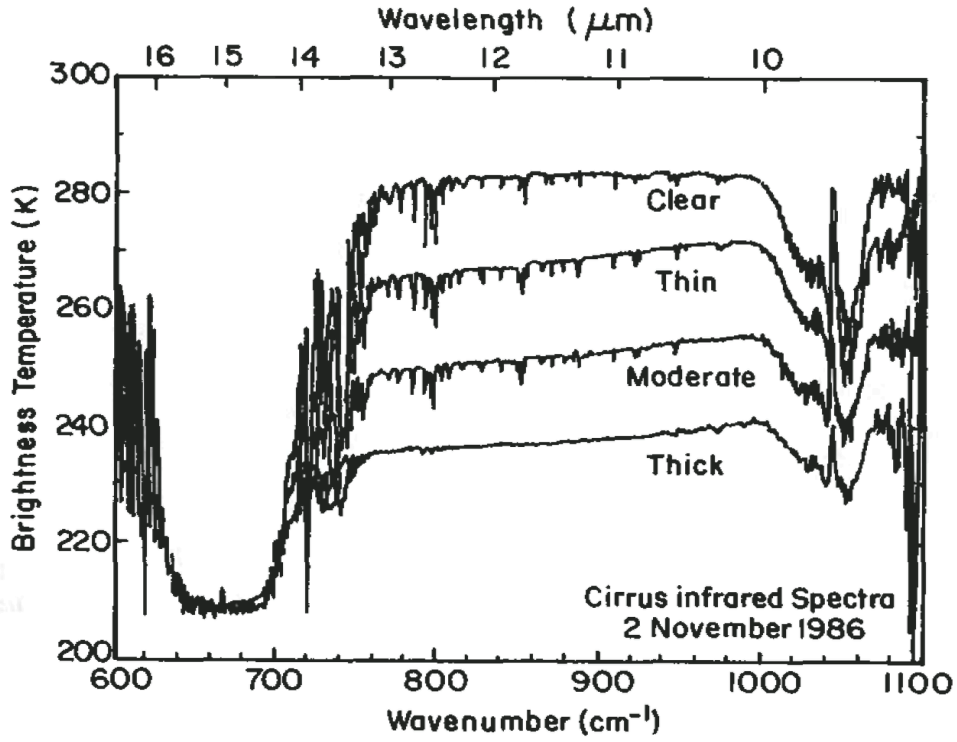

Clouds generally Decrease TB's, but depends STRONGLY on their cloud top temperature

Information about the atmosphere and surface are encoded in these emission spectra

Extract this information requires a simple model that can simulate the measurement

2. Sea surface temperature: split window approach

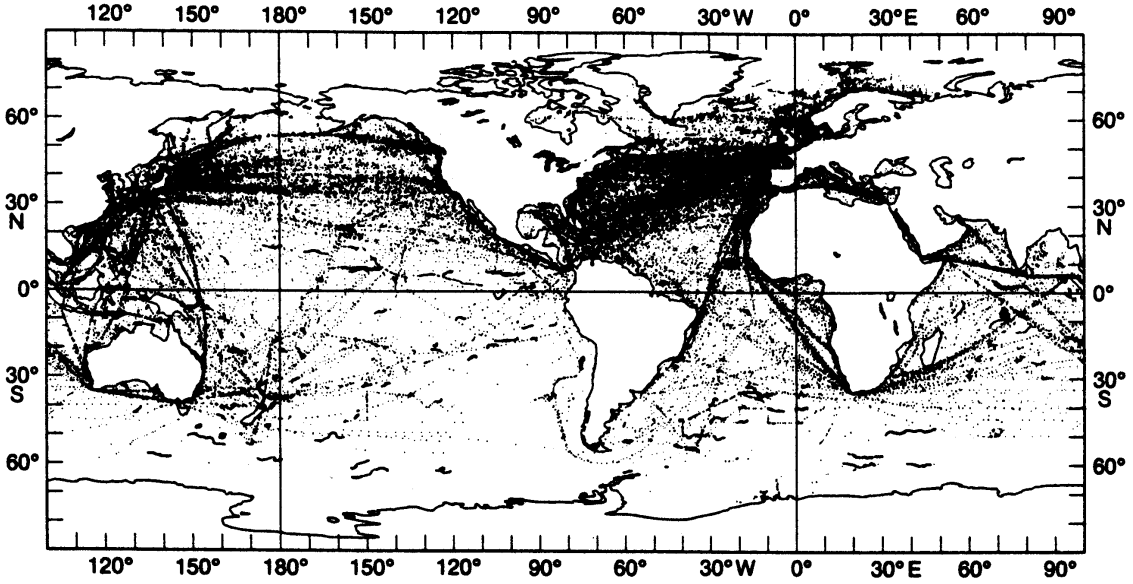

Table 3.1 Atmospheric Corrections to SST

T_s K	r_s^+ g/kg	k_2^* (cm^2/g/atm)	β	ΔT_s (K)
283	5.4	12.8	0.088	0.7
288	7.6	11.5	0.155	1.2
293	10.2	10.4	0.258	1.7
298	13.6	9.6	0.422	3.1
303	18.4	8.9	0.720	5.0

$^+$Assumes 70% relative humidity at the surface. * The absorption coefficient in the continuum may be approximated by $k = k_2 e$ where e is the water vapor partial pressure. For the definition of the absorption coefficient, see problem 3.12 and refer to Problem 7.10 for a definition of β–after Houghton and Lee (1972).

$$I_\lambda(\tau,\mu) = I_\lambda(\tau^*,\mu)e^{-(\tau^*-\tau)/\mu} + \int_\tau^{\tau^*} B_\lambda(t)\, e^{-(t-\tau)/\mu}\, \frac{dt}{\mu}$$

$$I(\tau = 0,\mu) = B(T_s)t^* + B(T_a)[1 - t^*]$$

Measure at two (window) wavelengths

$$I_1(\tau = 0, \mu) = B_1(T_s)Tr_1(\tau^*, \mu) + B_1(T_a)[1 - Tr_1(\tau^*, \mu)]$$

$$I_2(\tau = 0, \mu) = B_2(T_s)Tr_2(\tau^*, \mu) + B_2(T_a)[1 - Tr_2(\tau^*, \mu)]$$

assume

$T_{a1} = T_{a2} = T_a$ Assume Single Atmospheric Emitting temperature

also

$$B(T) \approx B(T_a) + \frac{dB}{dT}(T - T_a)$$ Taylor-expand about T_a

and

$$B_2(T) \approx B_2(T_a) + \frac{dB_2 / dT}{dB_1 / dT}(B_1(T) - B_2(T_a))$$

$$\eta = \frac{1 - t_1^*}{t_1^* - t_2^*}$$

$$B_1(T_s) = I_1 + \eta[I_1 - B_1(Tb_2)]$$

$$T_s \approx Tb_1 + \eta(Tb_1 - Tb_2)$$

$$SST = aT_{11} + b(T_{11} - T_{12}) + c$$

Multiple Channel Sea Surface Temperature (MCSST)

Two Unknowns: Sea Surface Temperature (SST), water vapor absorption

$$SST = T_i + \gamma(T_i - T_j) \qquad \gamma \rightarrow \text{water vapor absorption}$$

Types of MCSST's

Algorithm Name	Thermal Bands	Day/Night usage
Dual Window	3.7 and 11 µm	Daytime
Split Window	11 and 12 µm	Day and Night
Triple Window	3.7, 11, and 12 µm	Daytime

- 3.7 < 11 < 12 in terms of water vapor absorption
- 3.7 is affected by sunlight and generally not used in daytime measurements

Split Window Example

- Both blue and red curves are Top of Atmosphere Radiance computed with same parameters except the Blue(high humidity) is perturbed by 3x's

Surface Temp=292.8

	11 µm (K)	12µm (K)
MODIS humid	287.74	286.44
MODIS dry	290.43	289.89

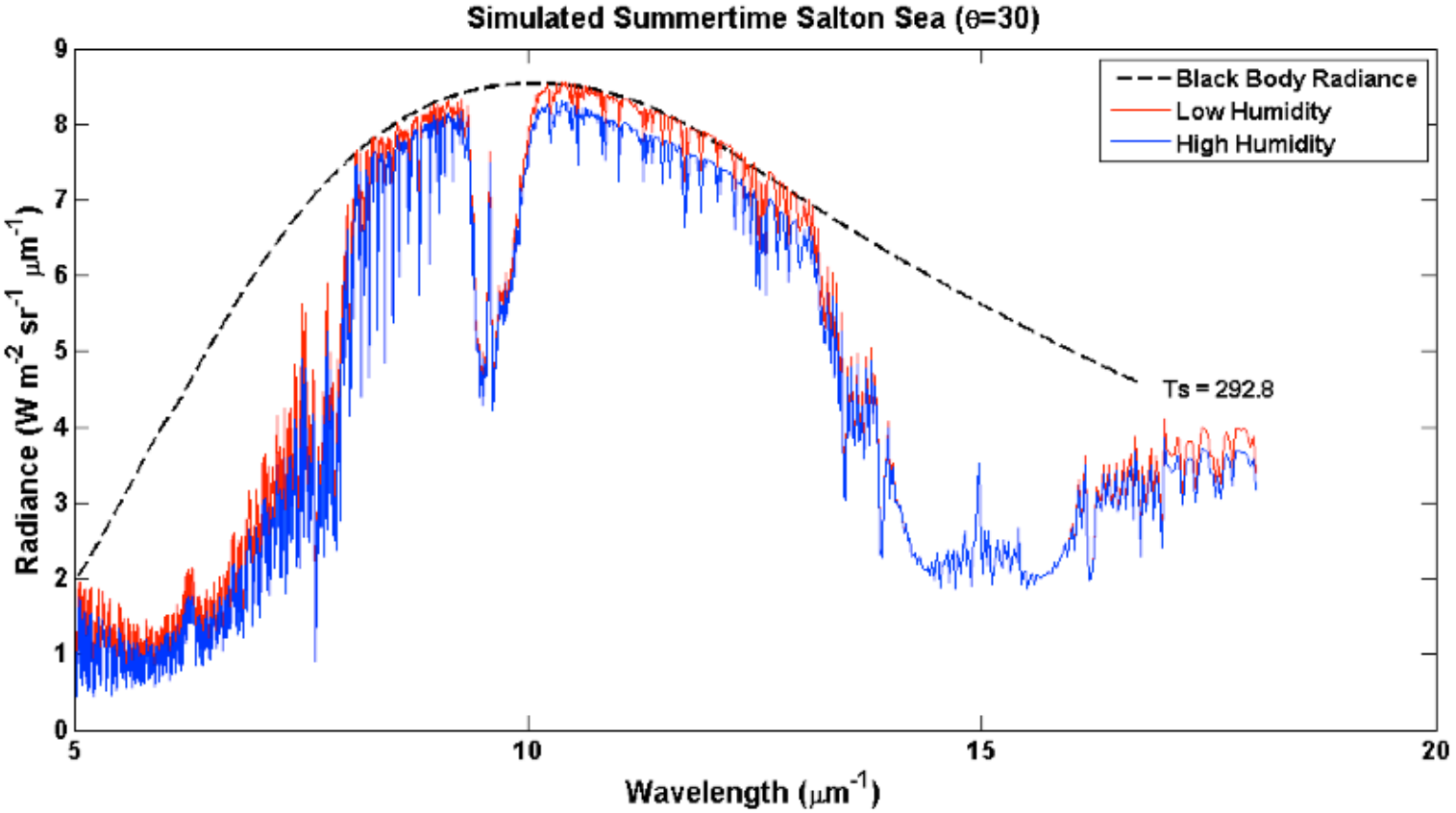

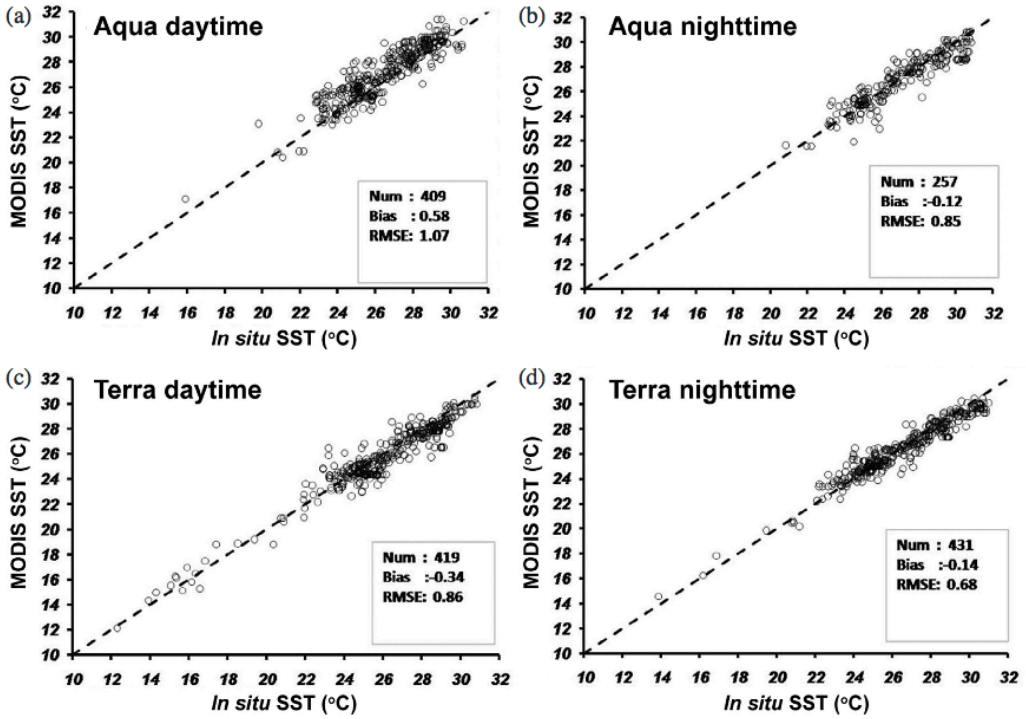

Idea is to tune the coefficients to actually bulk SSTs as measured by ships and bouys to remove contaminating effects of atmosphere – use satellite and *in situ* to produce merged product

Example SST map

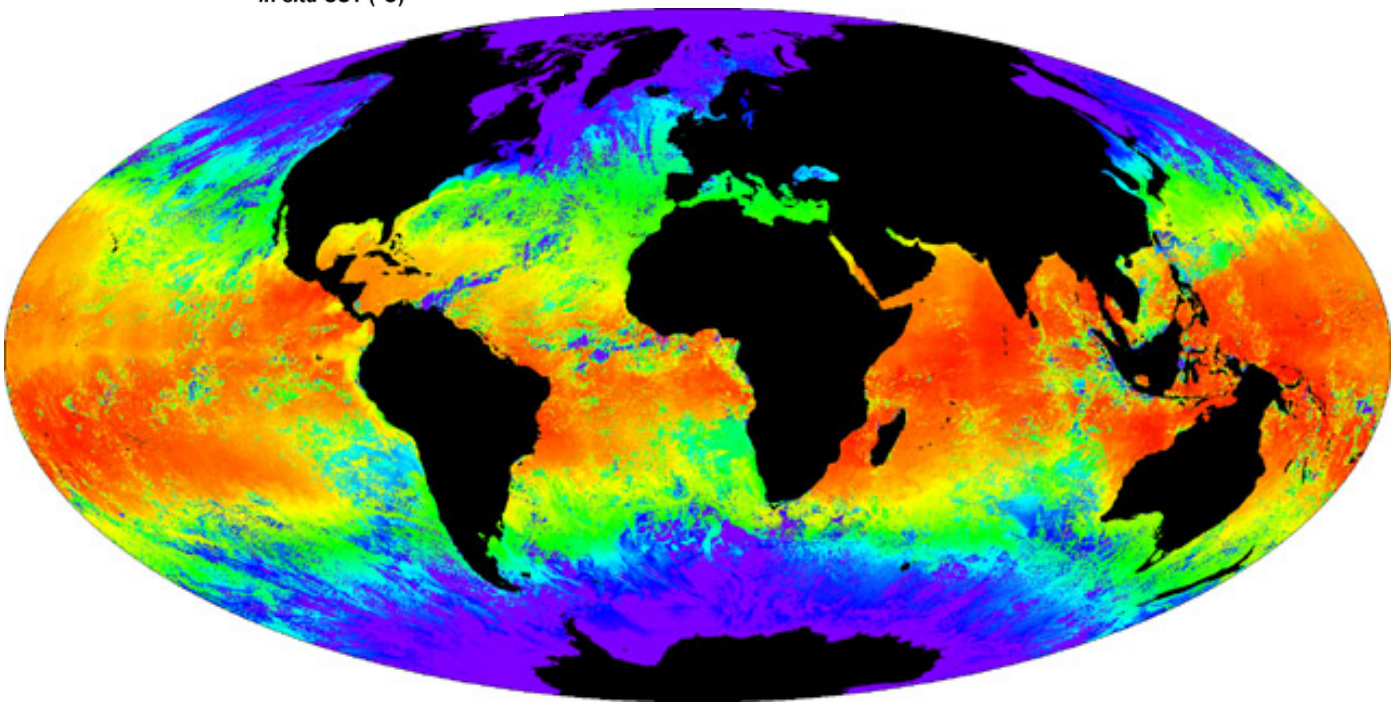

A Real-Time Global Sea Surface Temperature Analysis

RICHARD W. REYNOLDS

Climate Analysis Center, NMC/NWS/NOAA, Washington, DC

(Manuscript received 7 May 1987, in final form 25 August 1987)

ABSTRACT

A global monthly sea surface temperature analysis is described which uses real-time in situ (ship and buoy) and satellite data. The method combines the advantages of both types of data: the ground truth of in situ data and the improved coverage of satellite data. The technique also effectively eliminates most of the bias differences between the in situ and satellite data. Examples of the method are shown to illustrate these points.

Sea surface temperature (SST) data from quality-controlled drifting buoys are used to develop error statistics for a 24-month period from January 1985 through December 1986. The average rms monthly error is 0.78°C; the modulus of the monthly biases (i.e., the average of the absolute value of the monthly biases) is 0.09°C.

- Blends AVHRR SST with in-situ (ships+buoys)
- 3-channel at night, 2-channel during the day
- In-situ is used to correct for biases in infrared
- One version incorporates AMSR-E since 2002

Upper tropospheric humidity

Measurements in that part of the spectrum dominated by water vapor emission can be used to infer water vapor

Present-day sounders have channels located in the 6.3 um water vapor band (e.g channel 12 of TOVS) and channels on the 182 GHz water vapor line (e.g. SSMT2 & AMSUB)

Also equivalent to channel 12 of TOVS is part of the imager radiometers on geostationary satellites

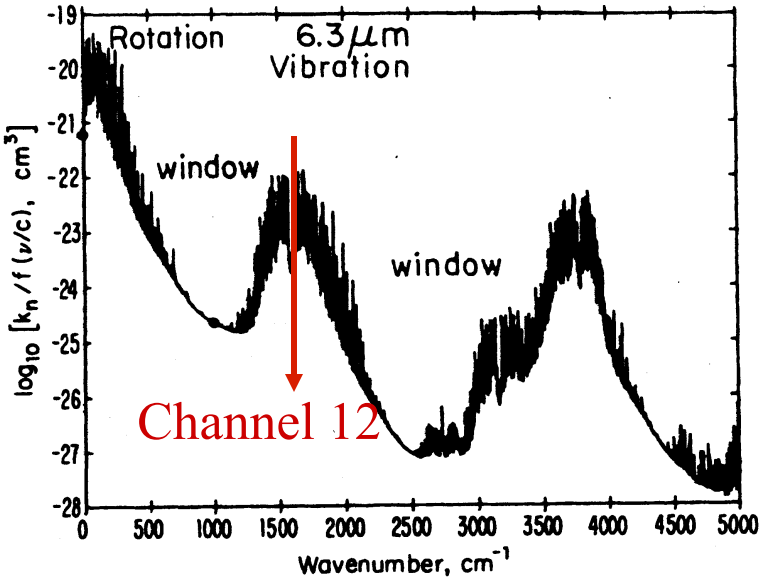

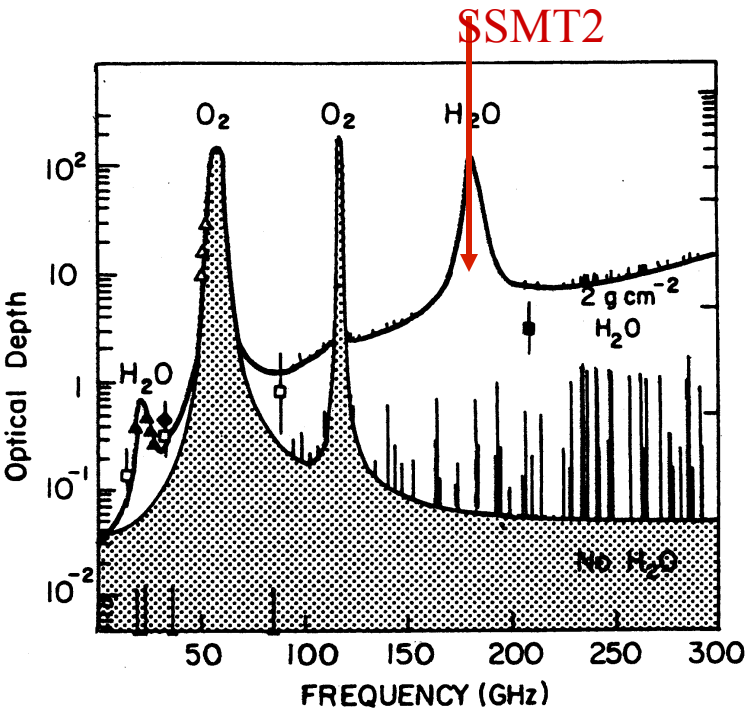

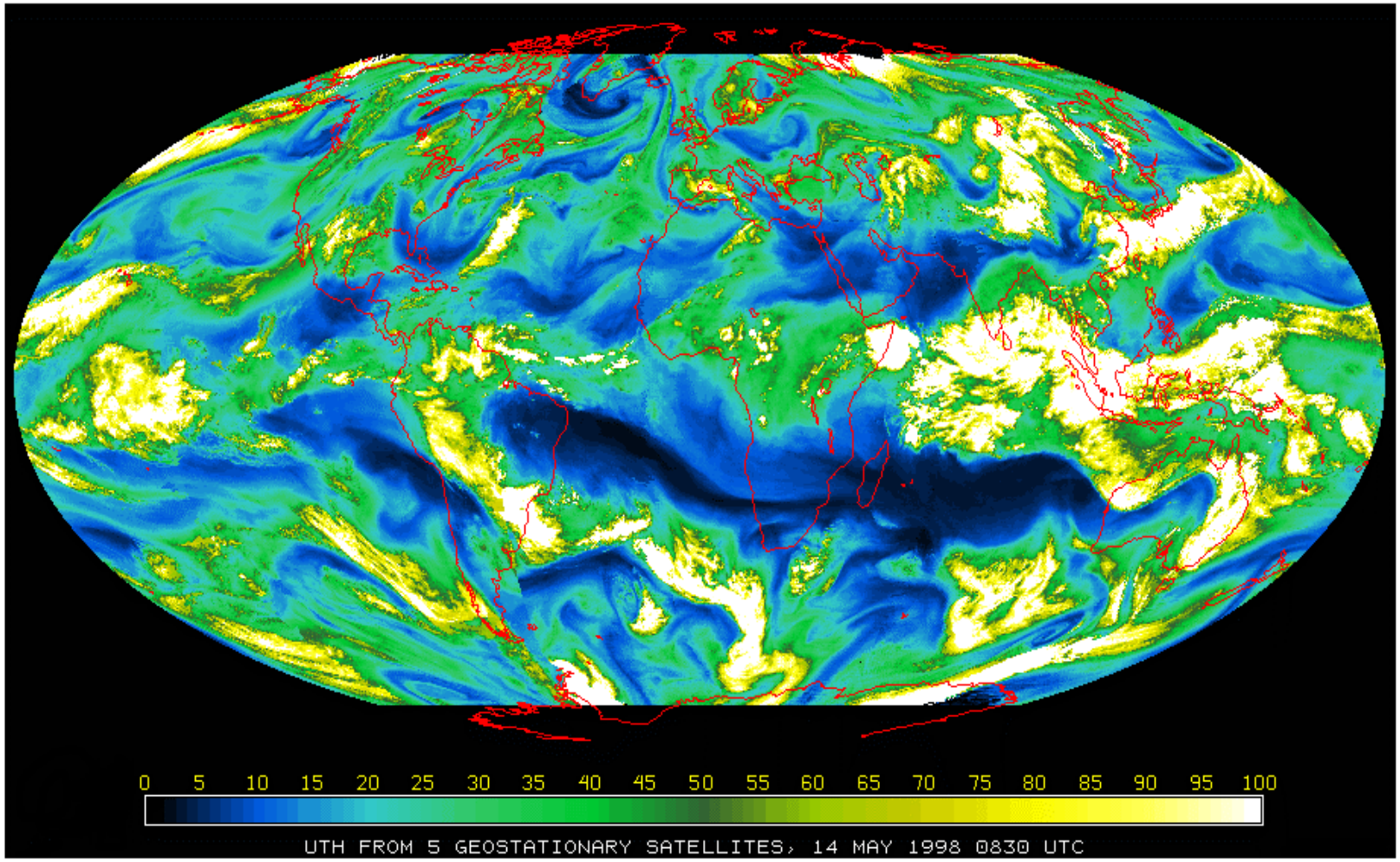

Upper tropospheric humidity from simultaneous observations

EUMETSAT

Early Humidity Weighting Functions

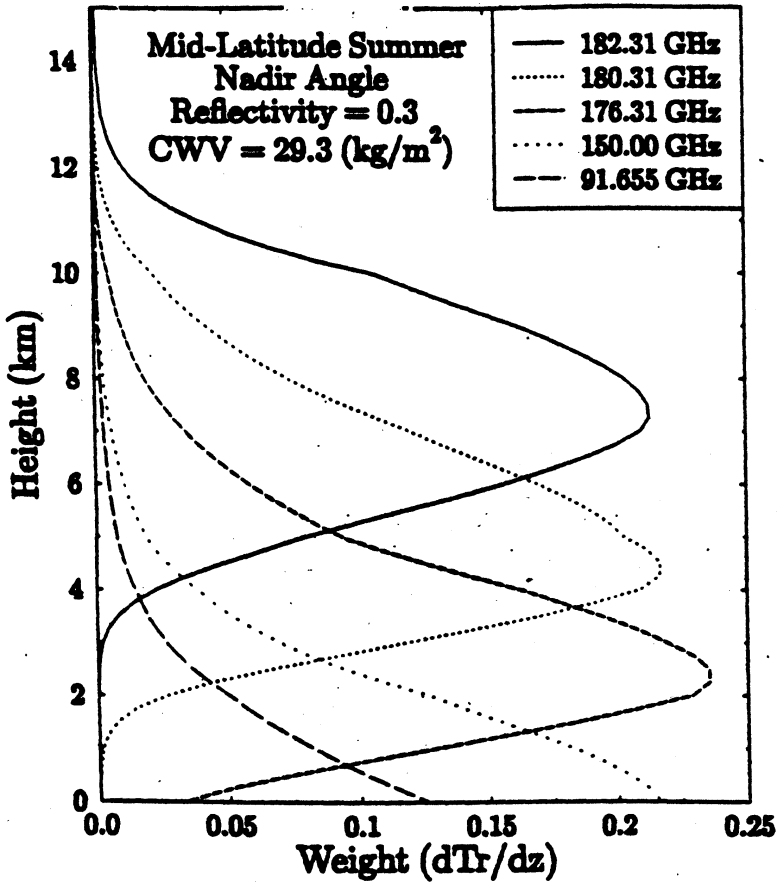

SSMT2

TOVS ch12

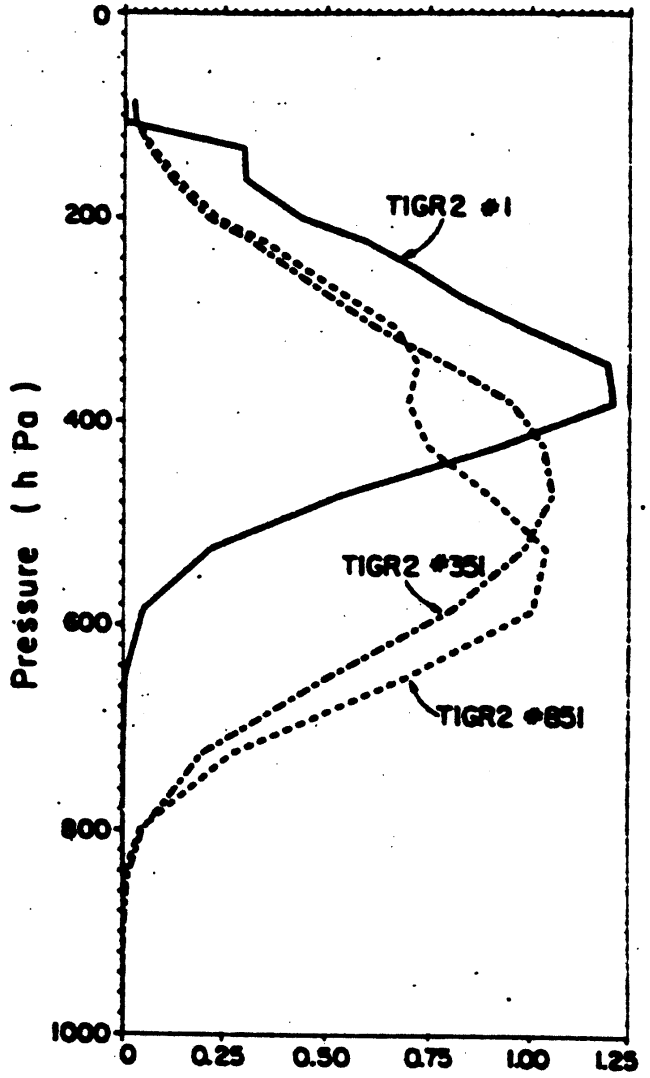

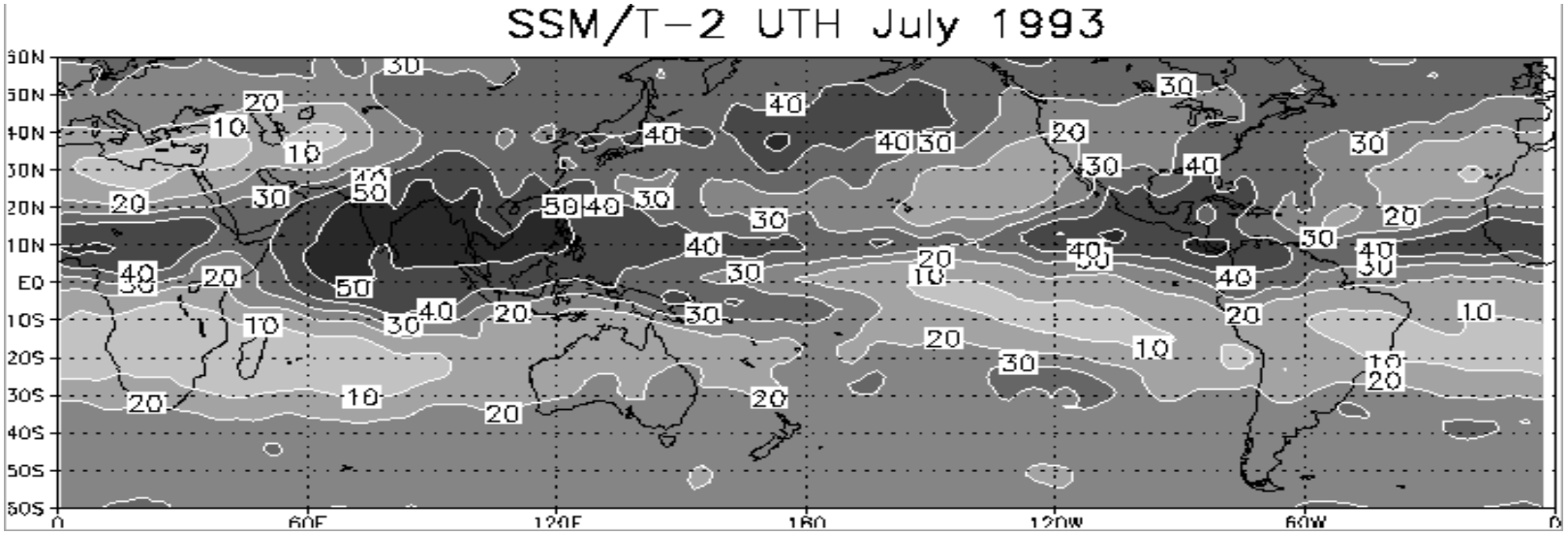
SSM/T-2 UTH July 1993
60N
50N
40N
30N
20N
10N
EQ
10S
20S
30S
40S
50S
0
60E
120E
180
120W
60W
0

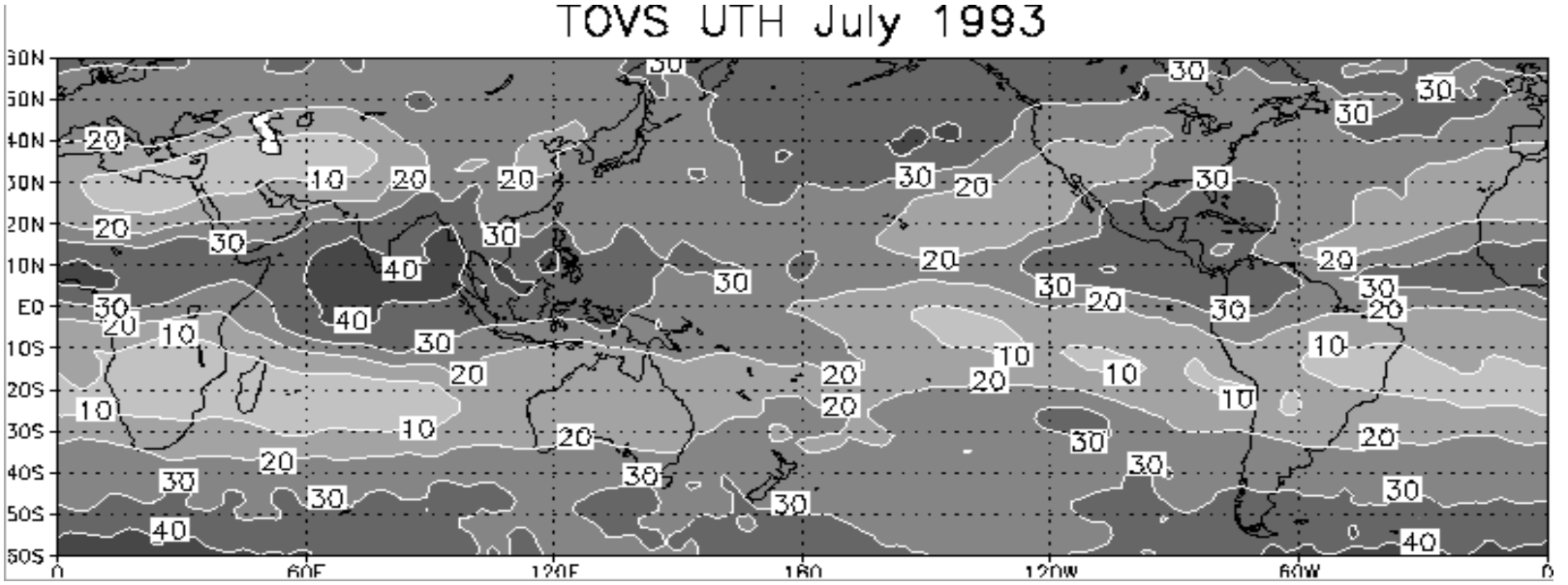
TOVS UTH July 1993
60N
50N
40N
30N
20N
10N
EQ
10S
20S
30S
40S
50S
0
60E
120E
180
120W
60W
0

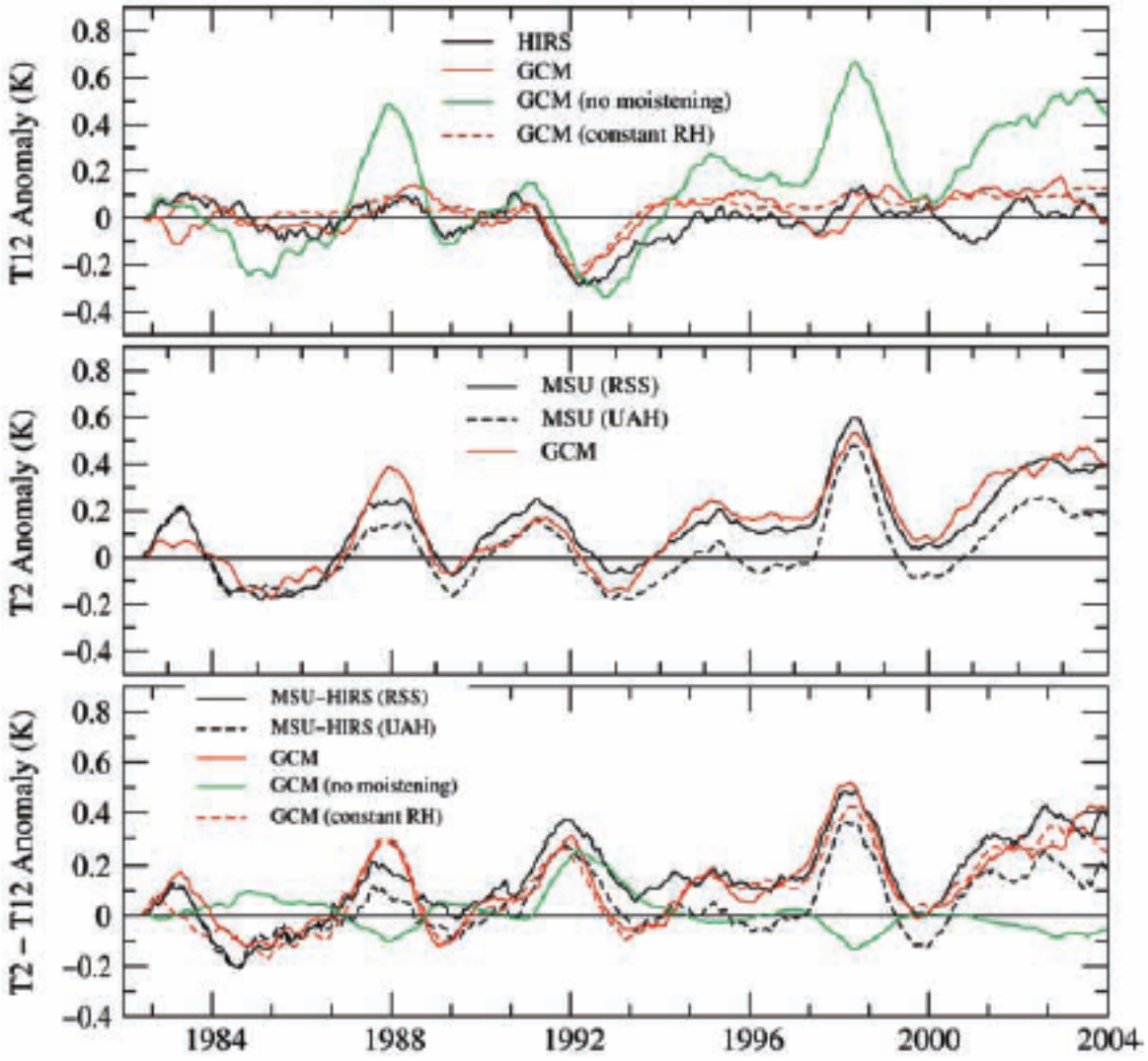

Fig. 2. Global mean time series of T12 (top), T2 (middle), and T2 – T12 (bottom) from GCM simulations (red) and satellite observations (black). The model-simulated radiances are also shown from calculations using a seasonally varying climatological profile with no moistening trend [green line (*21*)] and a prescribed moisture profile that moistens at a constant relative humidity rate [red dashed line (*21*)]. All time series are smoothed with a 6-month running mean.

Soden et al., 2005

AIRS onboard of AQUA

- NASA's EOS spacecraft
- Aqua launched May 4, 2002
- 705 km orbit (polar-orbiting)
- Early afternoon (1:30 PM) equator crossing time heading north
- AIRS system on Aqua:

→ AIRS (Atmospheric infrared Sounder)
→ AMSU-A (Advanced Microwave Sounding Unit)
→ HSB (Humidity Sounder Brazil)

- Other instruments:

→ MODIS (Moderate Resolution Imaging Spectroradiometer)

→ AMSR-E (Advanced Microwave Scanning Radiometer for EOS)

→CERES (Clouds and the Earth's Radiant Energy System)

AIRS

Monitoring Earth's Atmosphere

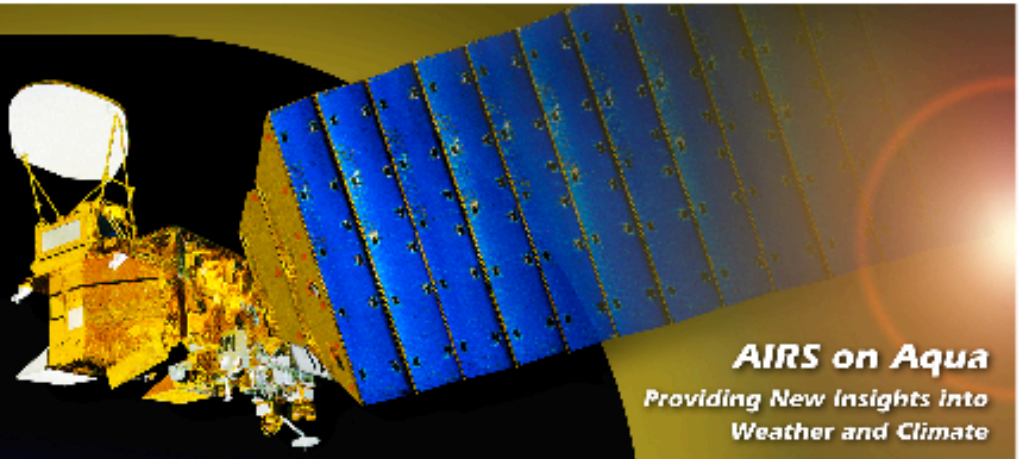

AIRS on Aqua

Providing New Insights into Weather and Climate

AIRS will:

Improve weather forecasting

Establish the connection between severe weather and climate change

Determine if the global water cycle is accelerating

Detect the effects of greenhouse gases

The Atmospheric Infrared Sounder, AIRS, brings climate research and weather prediction into the 21st century. From NASA's Aqua spacecraft, the AIRS instrument measures humidity, temperature, cloud properties, and the amounts of greenhouse gases. AIRS also reveals land and sea surface temperatures.

http://www.jpl.nasa.gov/airs

AIRS Spectral Coverage → Vertical Resolution

Jacobian matrix K=dBT/dX is the matrix of partial derivatives of the Brightness temperature with respect to the input parameter X. The weighting functions (=rows of K) reflect the relative contribution from each level to the total measured radiance.

Temperature weighting functions

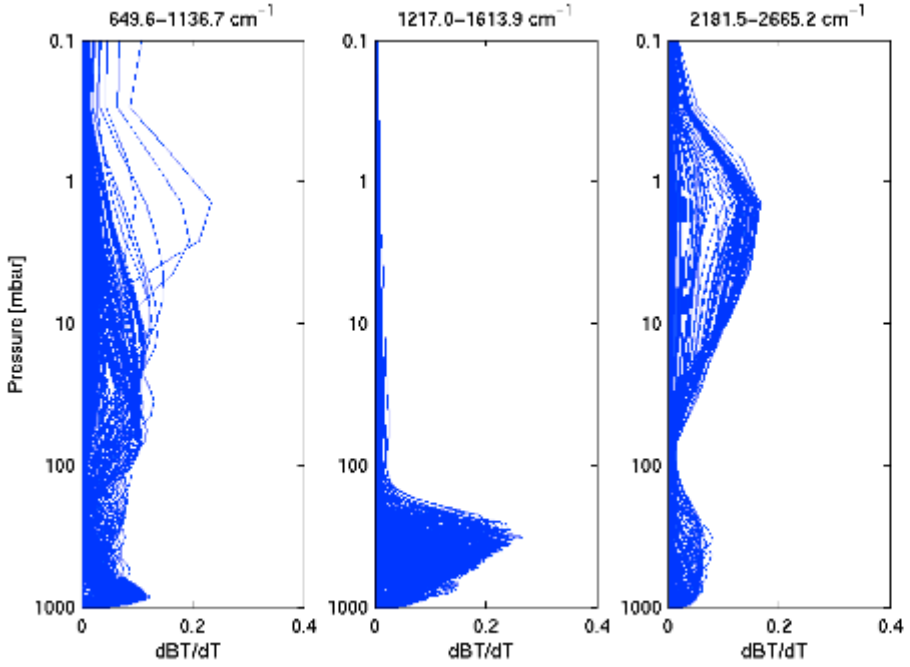

Humidity weighting functions

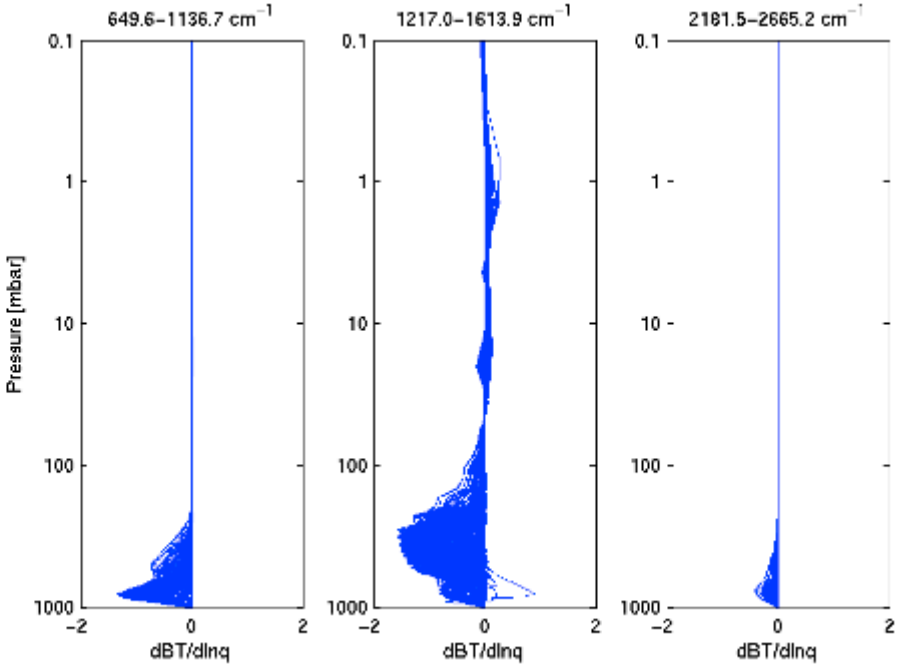

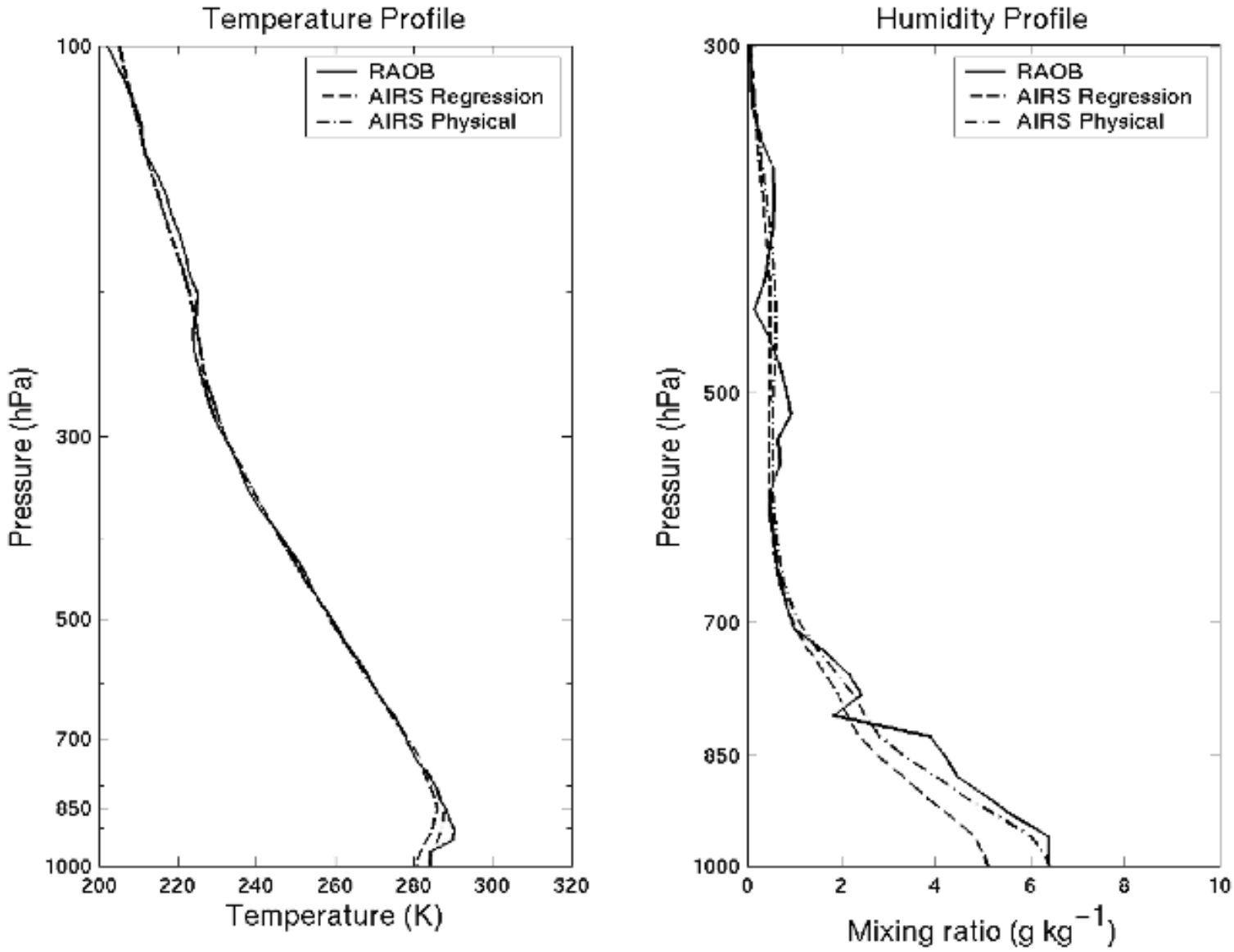

Fig. 4. Comparison of temperature (K) and mixing ratio on 9 January 2003 from the single AIRS FOV retrieved profiles at the ARM CART site at 0744 UTC (AIRS Regression and Physical), and a RAOB. In this situation where the moisture is not smooth, the AIRS physical retrieval captures the vertical structure fairly well.

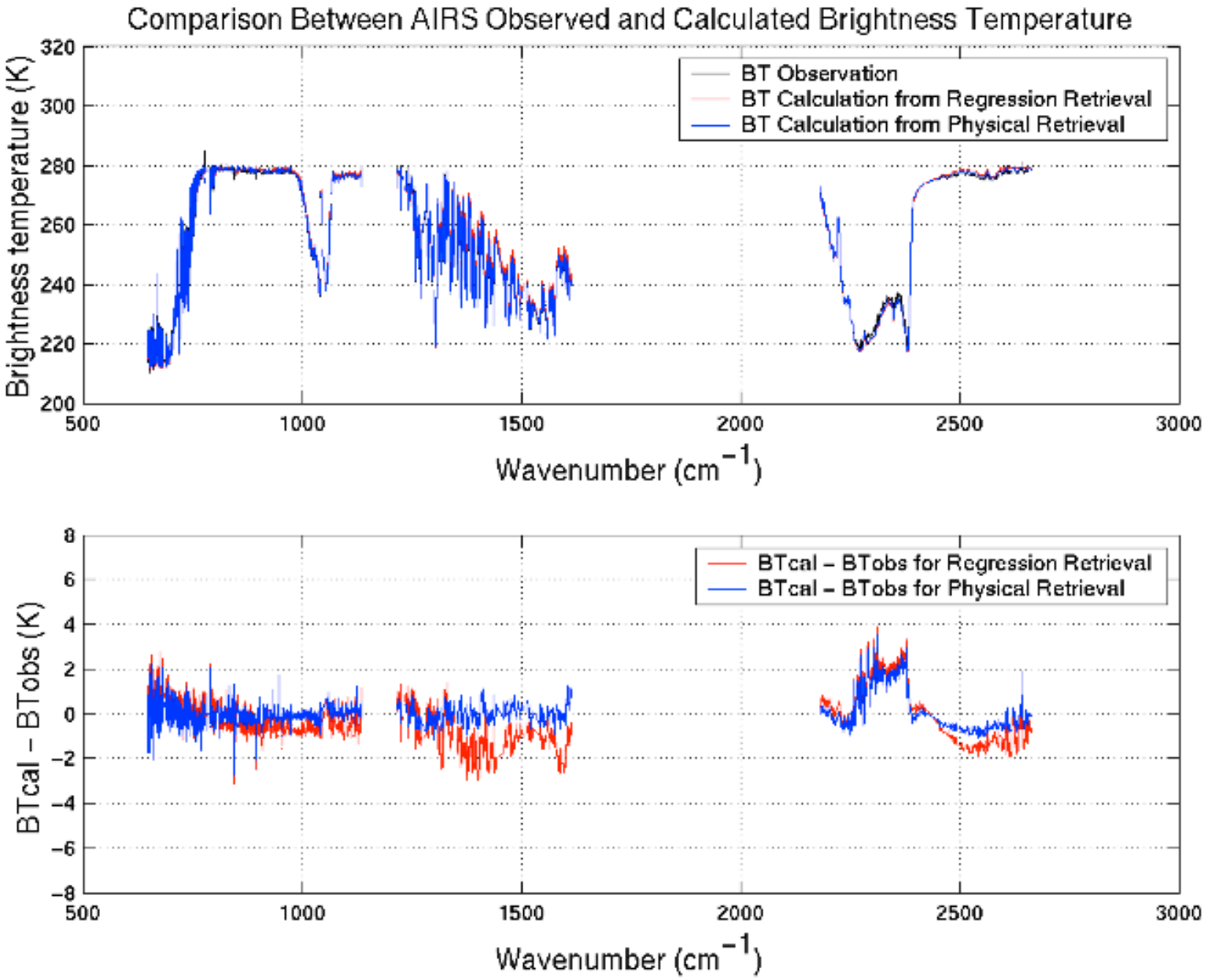

Fig. 5. Comparison between AIRS observed and calculated brightness temperature for the case in Fig. 4.

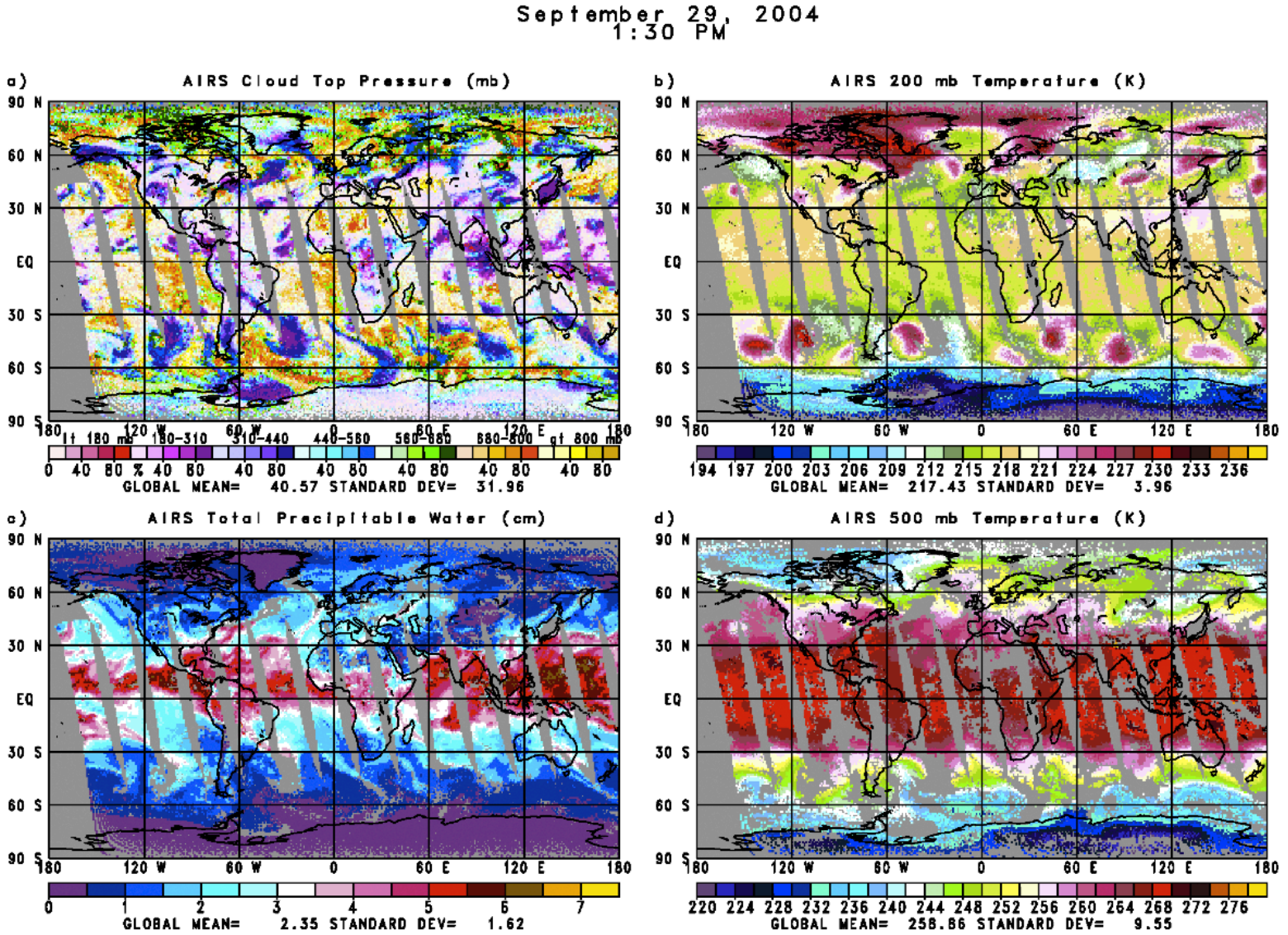
September 29, 2004
1:30 PM
a)
AIRS Cloud Top Pressure (mb)
lt 180 mb
180-310
310-440
440-560
560-680
680-800
gt 800 mb
0 40 80 % 40 80 40 80 40 80 40 80 40 80 40 80
GLOBAL MEAN= 40.57 STANDARD DEV= 31.96
b)
AIRS 200 mb Temperature (K)
194 197 200 203 206 209 212 215 218 221 224 227 230 233 236
GLOBAL MEAN= 217.43 STANDARD DEV= 3.96
c)
AIRS Total Precipitable Water (cm)
0 1 2 3 4 5 6 7
GLOBAL MEAN= 2.35 STANDARD DEV= 1.62
d)
AIRS 500 mb Temperature (K)
220 224 228 232 236 240 244 248 252 256 260 264 268 272 276
GLOBAL MEAN= 258.86 STANDARD DEV= 9.55
90 N
60 N
30 N
EQ
30 S
60 S
90 S
180
120 W
60 W
0
60 E
120 E
180

Weighting Functions

- Sensitivity of outgoing radiation to temperature or gas concentration at height z.

- Peak and width of weighting function determine which part of the atmosphere is sensed.

- Temperature weighting functions are linear (in principle).

- Gas weighting functions are non-linear.

Radiative Transfer for a Nadir Viewing Instrument

Recall upwelling radiative transfer equation:

$$I(\mu) = I(\tau_0, \mu)e^{-\tau_0/\mu} + \frac{1}{\mu}\int_0^{\tau_0} B(\tau)e^{-\tau/\mu}\, d\tau$$

Define transmission:

$$Tr(\tau,\mu) = e^{-\tau/\mu}$$

Derivative of transmission:

$$\frac{dTr}{d\tau} = -\frac{1}{\mu}e^{-\tau/\mu}$$

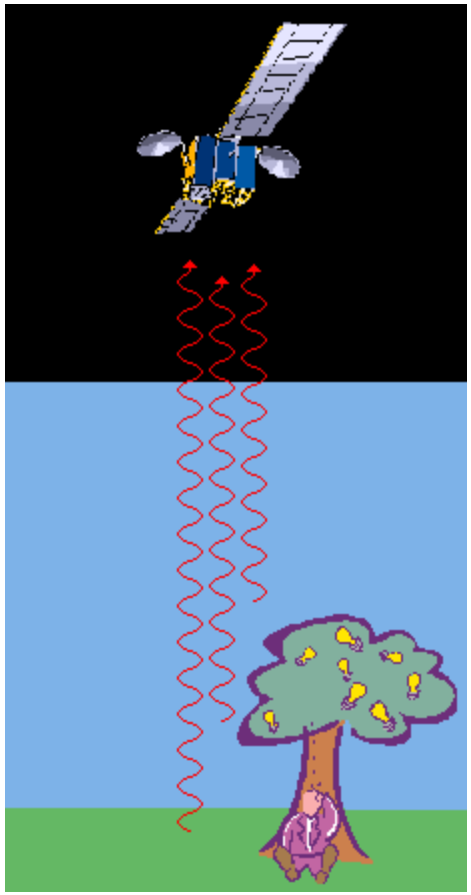

Weighting Functions for a Zenith Viewing Instrument

Recall upwelling radiative transfer equation:

$$I(\tau_0,\mu) = \frac{1}{|\mu|}\int_0^{\tau_0} B(\tau) e^{-(\tau_0-\tau)/|\mu|}\, d\tau$$

Transmission:

$$Tr(\tau,\mu) = e^{-(\tau_0-\tau)/|\mu|}$$

$$\vdots$$

$$Tr(\tau,\mu) = \exp\left[-\tau_0 + \tau_0 e^{-2z/H}\right]$$

Weighting function:

$$W(z,0) = \frac{dTr}{dz} = -\frac{2\tau_0}{H} e^{-\tau_0} \exp\left[-\frac{2z}{H} + \tau_0 e^{-2z/H}\right]$$

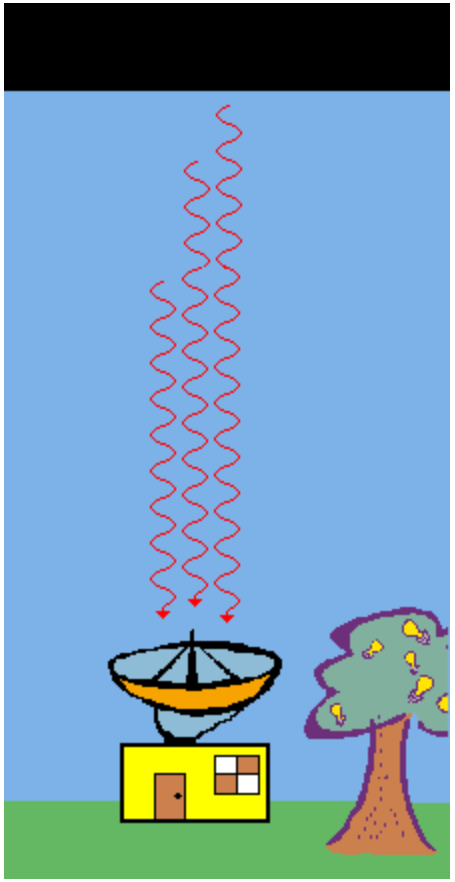

Comparison:

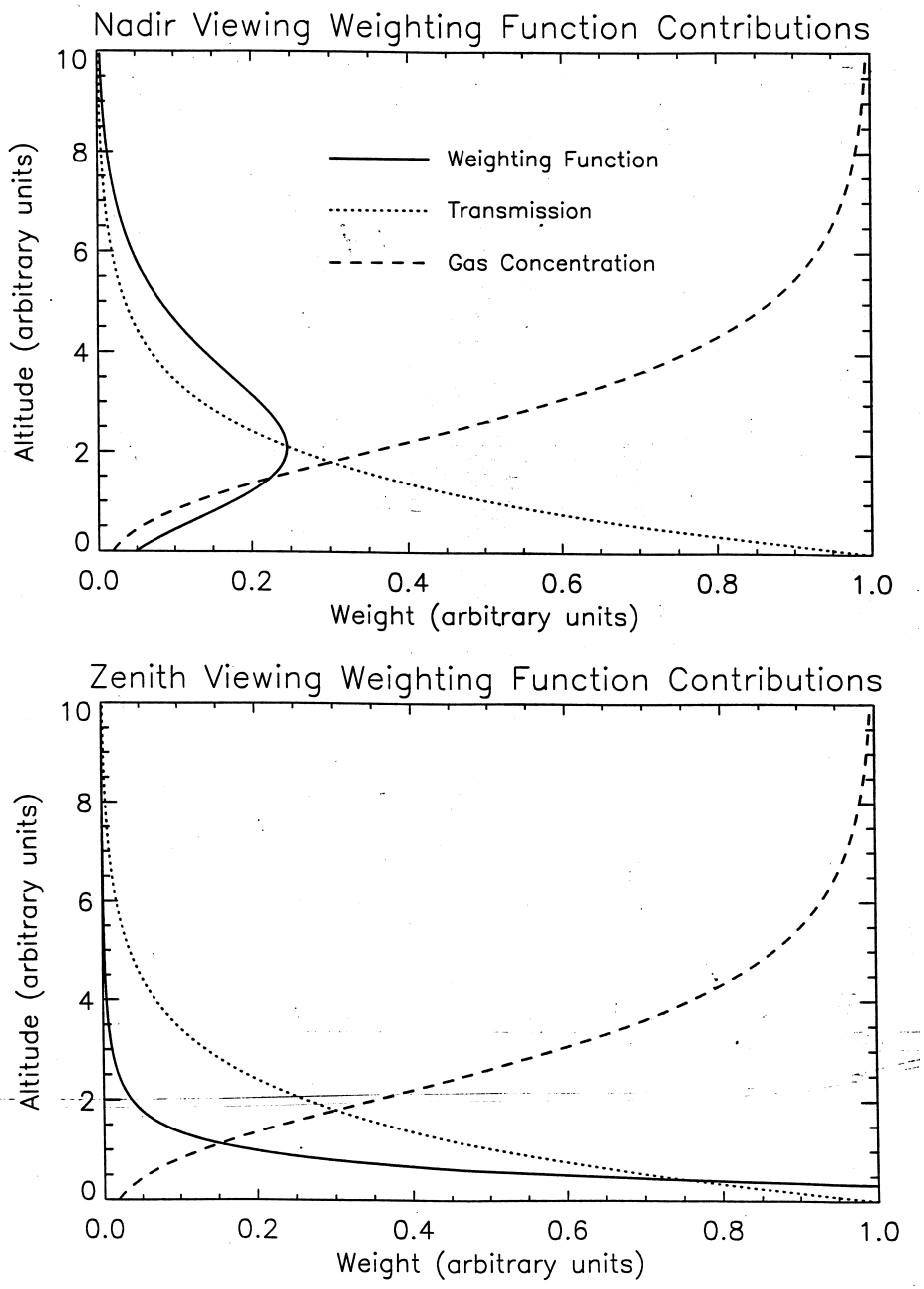
Nadir Viewing Weighting Function Contributions
Weighting Function
Transmission
Gas Concentration
Altitude (arbitrary units)
Weight (arbitrary units)
0
2
4
6
8
10
0.0
0.2
0.4
0.6
0.8
1.0
Zenith Viewing Weighting Function Contributions
Altitude (arbitrary units)
Weight (arbitrary units)

Weighting Functions for Limb Sounding

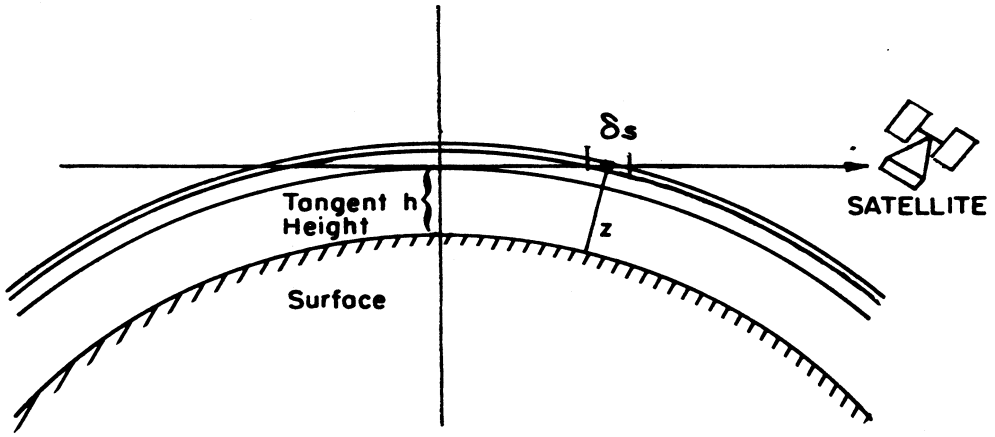

Figure 7.17 Limb viewing geometry. The satellite instrument scans through the atmosphere along the limb at a tangent height h. Intensity is received from segments δs of the path at height z.

Radiative transfer equation:

$$I(h) = \int_{\infty}^{0} B(s) \frac{\partial \mathrm{T}(\mathrm{s},0)}{\partial s} ds$$

where $s \approx 2R(z-h)$ is the path through the atmosphere.

…following pp. 361-363 of the text,

$$W(h;z,\infty) = \tau^* \sqrt{R/2(z-h)}\, e^{-2z/H}\left[e^{-\tau_1} + e^{-\tau_2}\right]$$

where,

$$\tau_1 = \frac{\tau^*}{2}\sqrt{\pi HR}\left[1 - erf\left(\sqrt{2(z-h)/H}\right)\right]e^{-2h/H}$$

$$\tau_2 = \tau_1 + \tau^* \sqrt{\pi HR}\, erf\left(\sqrt{2(z-h)/H}\right)e^{-2h/H}$$

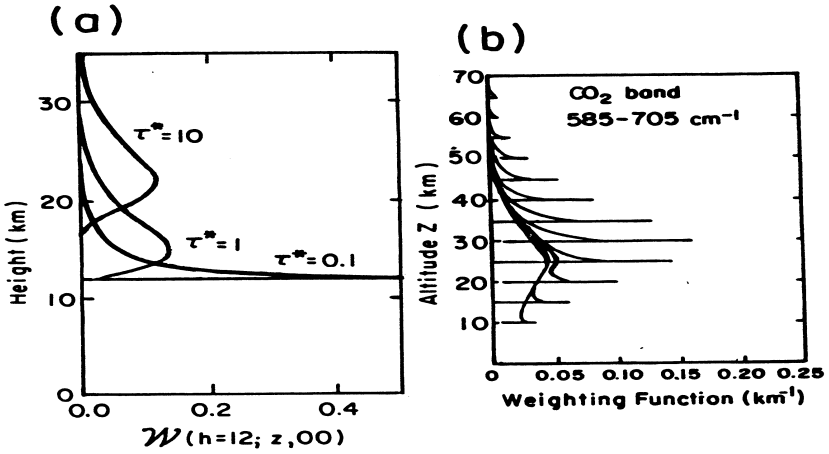

Figure 7.18 (a) The weighting function for limb sounding derived from (7.48) with H=7 km, R=6370 km, and h=12 km for three values of τ^*. (b) A set of weighting functions for a limb sounder based on the ideal case of an instrument with an infinitesimal vertical field of view. The weighting functions are computed for the spectral band 585–705 cm^{-1} which covers most of the 15 μm absorption band of carbon dioxide (after Gille and House, 1971).

- At low optical depth weighting functions are peaked close to the tangent height.

- At high optical depth weights are broader and closer to the satellite.

Advantages of Limb Sounding by Emission

•None of the emitted radiation seen by the satellite originates below the tangent height: allows for relatively high vertical resolution.

•The surface has no influence on the measured intensities.

•Due to the geometry of limb sounding, considerably more emitting gas is encountered along grazing paths than on straight ones increasing the instrument sensitivity to gases of low concentration.

•Also, due to paths being high in the atmosphere, effects of pressure broadening are reduced.

Disadvantages of Limb Sounding by Emission

•Very sensitive to aerosol in the lower stratosphere.

•Cannot be used in the troposphere because atmosphere is too optically thick.

Gas Weighting Functions

- In this case we're interested in the sensitivity of the radiance to changes in the gas concentration at each layer, not the contribution to the total radiance from each layer as before.
- Gas weighting functions are more complicated in practice because they depend on the potentially variable gas concentration itself.
- We define the weighting function with respect to a gas concentration *c(z)* as:

$$W_{gas}(z) = \frac{\partial I}{\partial c_z} = I_{surf}\frac{\partial t^*}{\partial c_z} + \int_0^\infty B(T)\frac{\partial}{\partial c_z}\left[\frac{\sigma_{gas}(z')c(z')N_{dry}(z')}{\mu}t(z',\infty)\right]dz'$$

But equally it can be defined in terms of the averaging kernel in the optimal estimation framework

$$\hat{\mathbf{x}} = \mathbf{A}\mathbf{x} + (\mathbf{I} - \mathbf{A})\mathbf{x}_a + \boldsymbol{G}\boldsymbol{\varepsilon}_y \qquad A_{ij} \equiv \frac{\partial \hat{x}_i}{\partial x_{true,j}}$$

Weighting Functions vs. Averaging Kernels

- A *weighting function* tells you the response of an individual measurement (a "channel") to a change in an underlying geophysical variable.

  eg: $\vec{W}_i = \frac{\partial y_i}{\partial \vec{T}}$ for channel *i*

- An *averaging kernel* tells you the response of the retrieved quantity for a change in the true quantity. For a given retrieved quantity, it is

  $\vec{A}_i = \frac{\partial \hat{T}_i}{\partial \vec{T}_{true}}$ for retrieved Temperature *I*

- The weighting function depends on the measurement system only, and is one per channel. The averaging kernel depends on the retrieval method as well, and generally incorporates many measurements into one AK

Averaging kernel : analogous to a weighting function

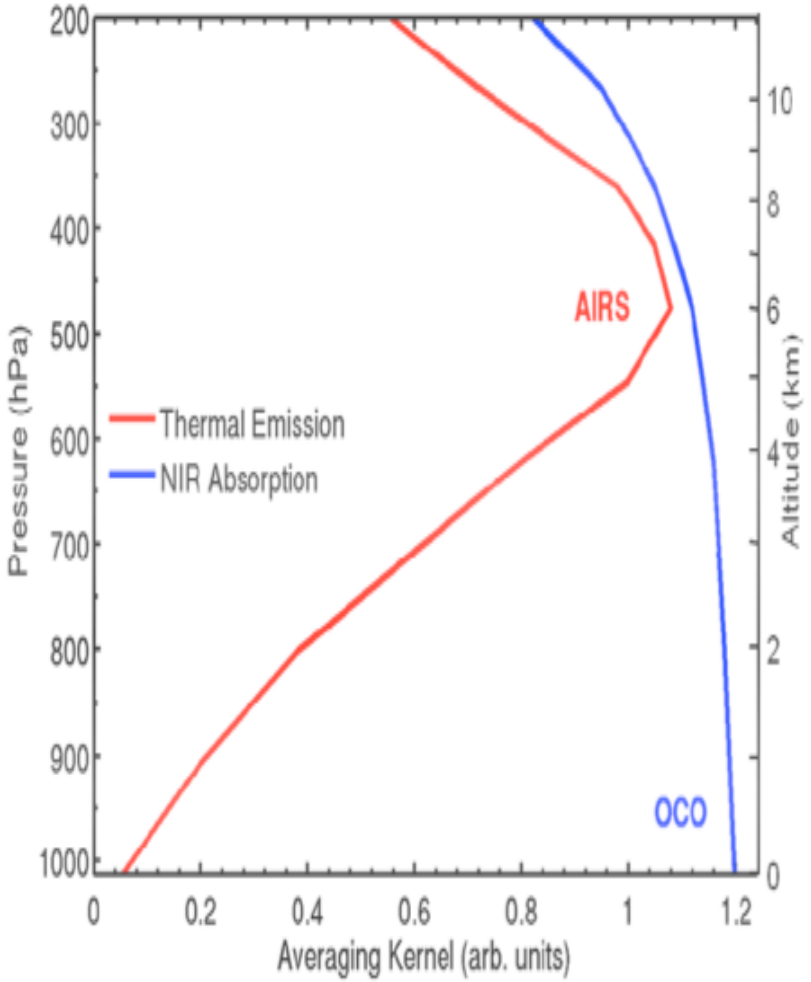

Averaging kernels for 1.61 µm CO2 band (blue) and thermal IR emission near 14.3 µm (red). (Crisp *et al.*, 2004; Chahine *et al.*, 2005).

NIR/IR retrieval of "column" CO_2

In the thermal IR, CO_2 information is spread through the troposphere whereas in the NIR CO_2 information is fairly uniform throughout the atmosphere.

TCCON Averaging Kernels

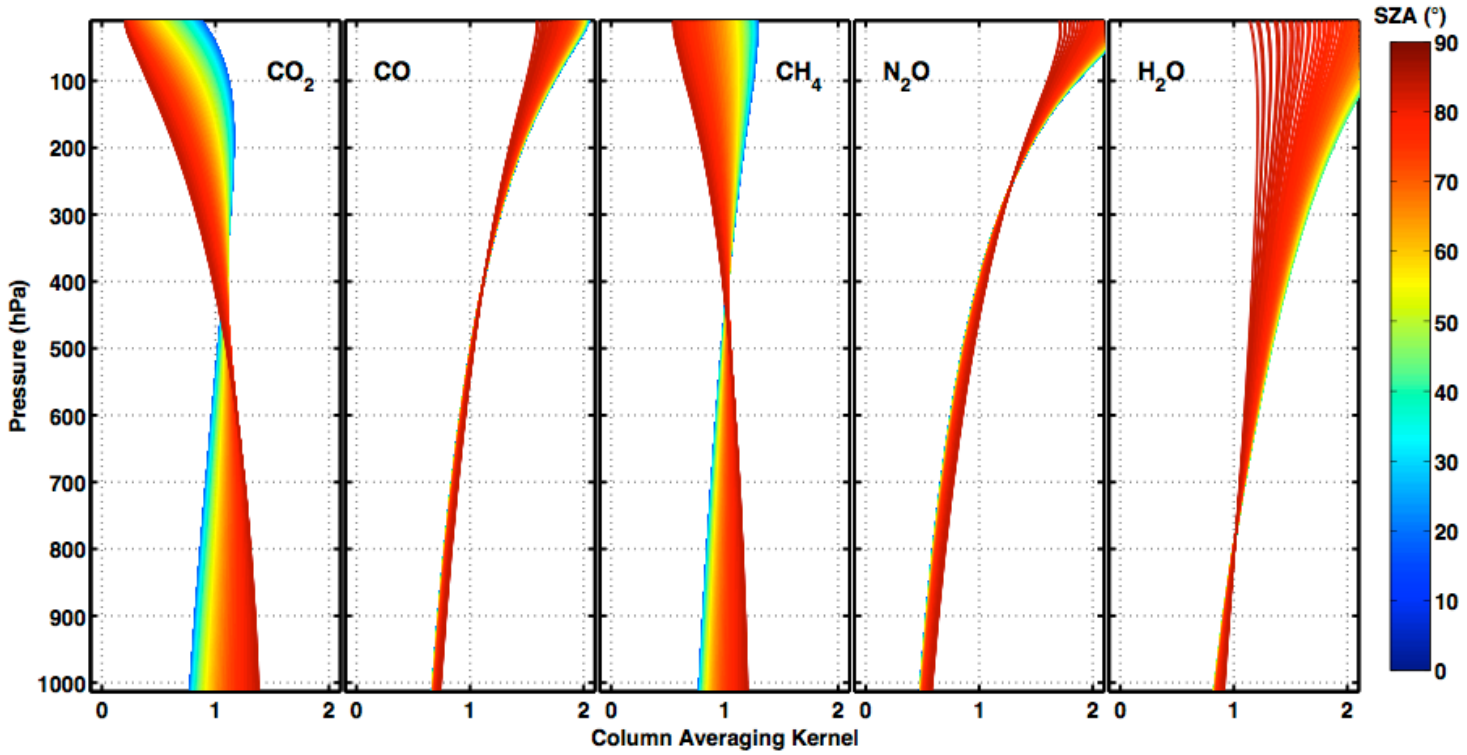

Fig. 3. Column averaging kernels for the Lamont TCCON site. The colors represent different solar zenith angles. Column averaging kernels for other TCCON sites are similar.

Averaging Kernels from Project 2

•oscillations

•very broad
•very small values along diagonal.

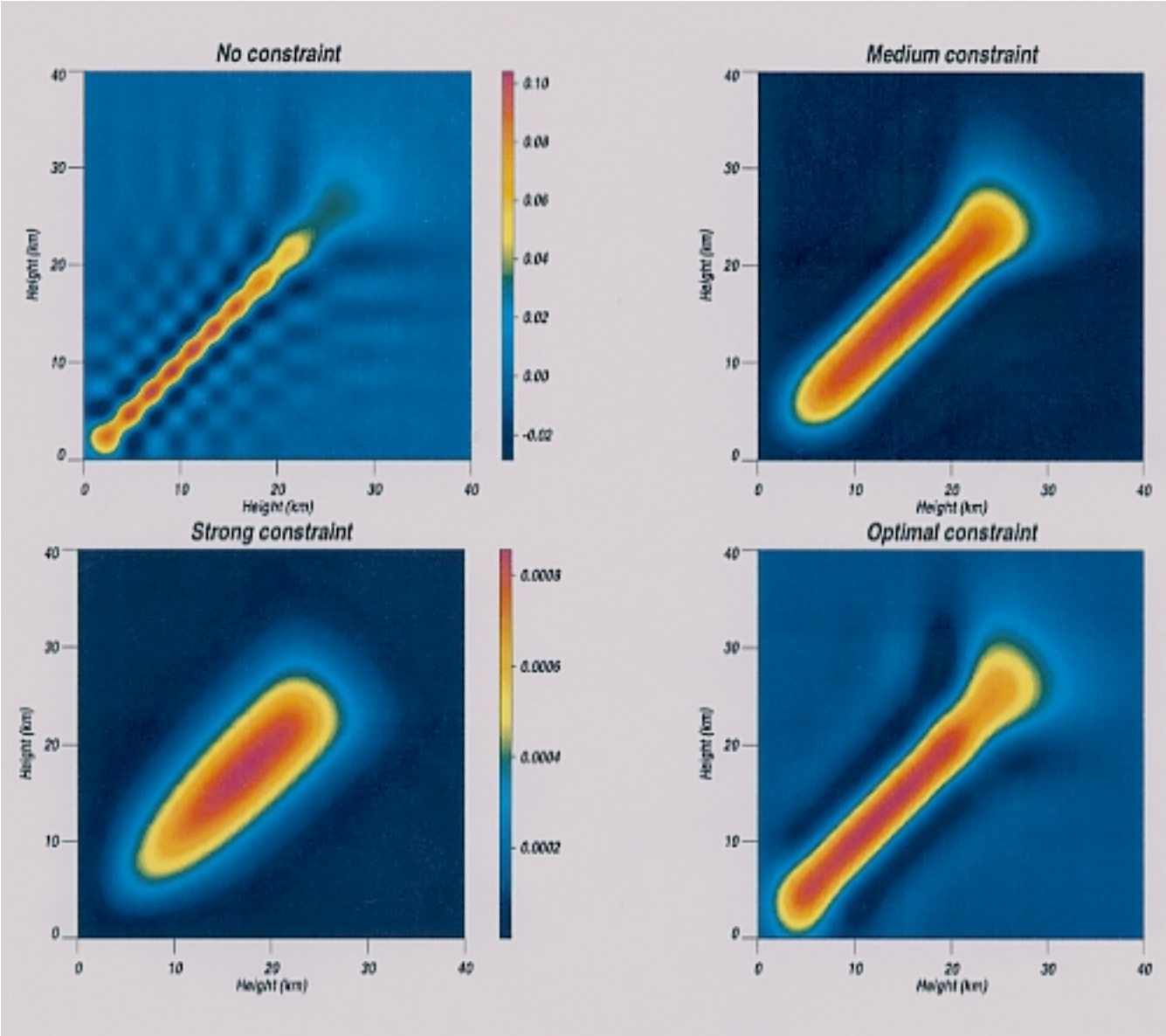

•broad especially at higher levels

•optimal solution
•almost diagonal
•no oscillations

TABLE I

SUMMARY OF MODIS PIXEL-LEVEL (LEVEL-2) CLOUD PRODUCTS AND THEIR CURRENT DEPENDENCIES. * TERRA DESIGNATION (AQUA IDs ARE MYD35, MYD06, ETC.); [a] NSIDC NISE AND/OR NCEP SEA ICE CONCENTRATION; [b] NCEP GDAS SIX-HOUR DATASET; [c] NCEP REYNOLDS BLENDED SST PRODUCT; [d] AGGREGATION of MODIS ECOSYSTEM CLASSIFICATION PRODUCT (MOD12) WITH MODIS DIFFUSE SKY SURFACE ALBEDO PRODUCT (MOD43). SEE TEXT FOR FURTHER DETAILS

Retrieved parameter	Earth Science Data Designation Product ID*	Investigators	MODIS spectral bands used	Spatial resolution (km)	MODIS ancillary input	Non-MODIS ancillary input
CLOUD MASK	**MOD35**	Ackerman *et al.*	up to 20 bands, VIS thru IR	0.25, 1		snow/sea ice mask [a]
CLOUD PROPERTIES	**MOD06**					
CLOUD TOP PROPERTIES						
Cloud-top pressure (p_c), cloud-top temperature (T_c), effective emissivity ($f\varepsilon$)		Menzel *et al.*	11 μm and CO_2 bands (31–36)	5	**MOD35**	model/assimilated T, p profiles [b], SST [c]
CLOUD OPTICAL AND MICROPHYSICAL PROPERTIES:						
Cloud optical thickness (τ_c), particle effective radius (r_e), water path		King *et al.*	VIS, NIR, SWIR, MWIR (bands 1, 2, 5, 6, 7, 20)	1	**MOD35, MOD06** (p_c, T_c), ecosystem + surface albedo[d]	snow/sea ice mask [a], model/assimilated T, p profiles [b], SST [c]
Thermodynamic phase (IR algorithm)		Baum *et al.*	8.5, 11 μm bands (bands 29, 31)	5		

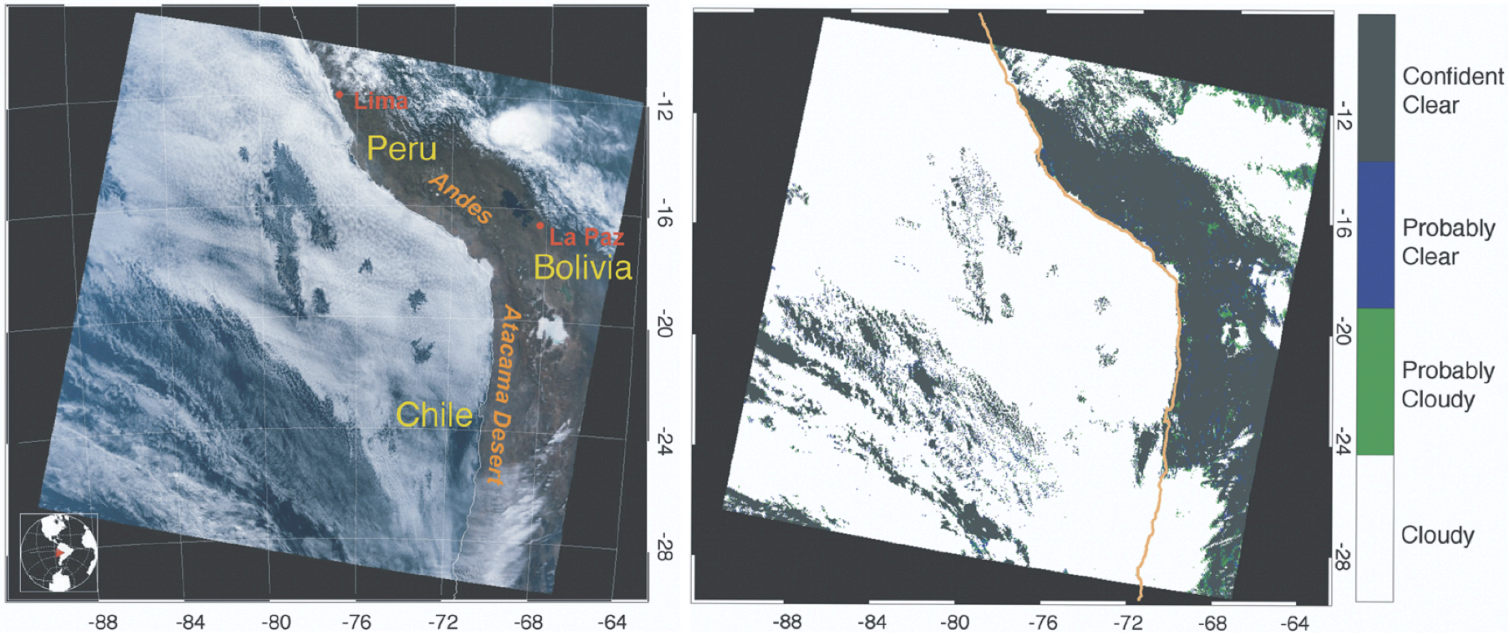
Lima
Peru
Andes
La Paz
Bolivia
Atacama Desert
Chile
-12
-16
-20
-24
-28
-88
-84
-80
-76
-72
-68
-64
Confident Clear
Probably Clear
Probably Cloudy
Cloudy

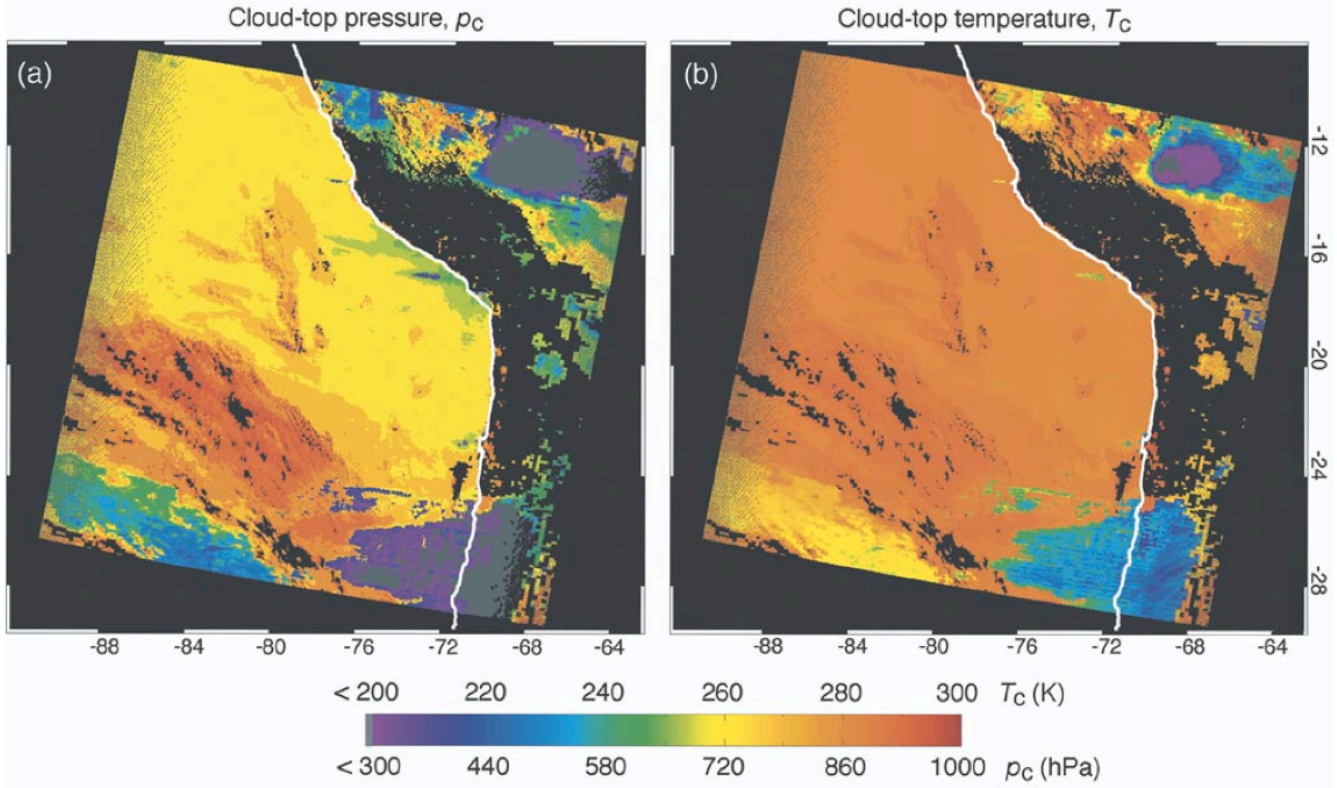
Cloud-top pressure, p_C
Cloud-top temperature, T_C
(a)
(b)
-12
-16
-20
-24
-28
-88
-84
-80
-76
-72
-68
-64
< 200
220
240
260
280
300
T_C (K)
< 300
440
580
720
860
1000
p_C (hPa)

"CO_2 Slicing" (Wylie & Menzel, 1989)

- Can determine cloud top pressure to within about 50 hPa
- Works best for single-layer clouds with top at or above 700 hPa.
- Relies on differential absorption within CO_2 bands near 15 μm. Use 2+ channels near this wavelength.
- Cloud-top height with MISR (stereographic) or CloudSat/Calipso (active ranging) are generally superior.

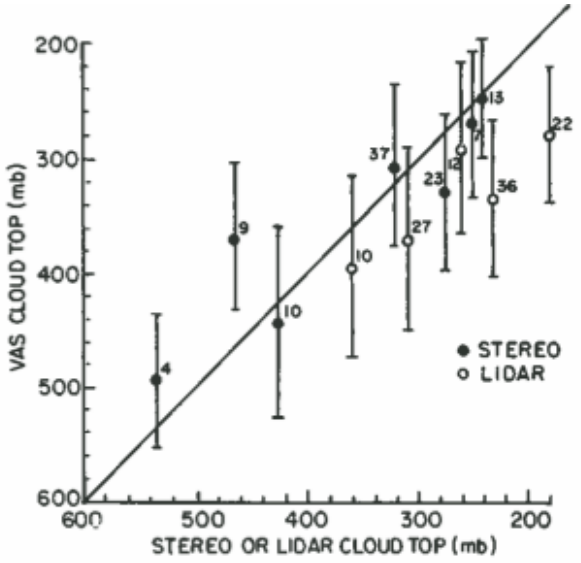

Fig. 7.28 The mean and standard deviation of all VAS cloud-top pressure data compared to lidar and satellite stereo cloud-top pressures. The error bars are 1 SD from the mean for the VAS derived pressures (Wylie and Menzel, 1989).

$$R(\eta) - R_{clr}(\eta) = -N\epsilon B[\eta, T(P_s)]\tau(\eta, P_s) - N\epsilon \int_{P_s}^{P_c} \{B[\eta, T(p)]d\tau/dp\}dp + N\epsilon B[\eta, T(P_c)]\tau(\eta, P_c). \quad (A3)$$

This is the cloud signal in the satellite measured radiances for spectral band η; it is the radiance difference of the cloudy FOV from neighboring clear FOVs. A simplified equation, after integration by parts, is

Information content in Microwave emission

- DMSP
  - multiple launches since 1987
  - 815-853 km polar orbits (one in morning and one in evening)
- Sensor characteristics
  - 7 channel microwave radiometer with frequencies at 19.35, 37.0, 85.5, 22.235(v)
  - conical scan mirror with 53.1° incident angle at Earth's surface
  - 25 km resolution (12.5 km - 85 GHz)
- Geophysical Parameters (accuracy)
  - wind speed (~1-1.6 m/s)
  - column water vapor (~1.2 mm)
  - column liquid water (~0.025 mm)
  - column rain rate (0.3 km*mm/hr)

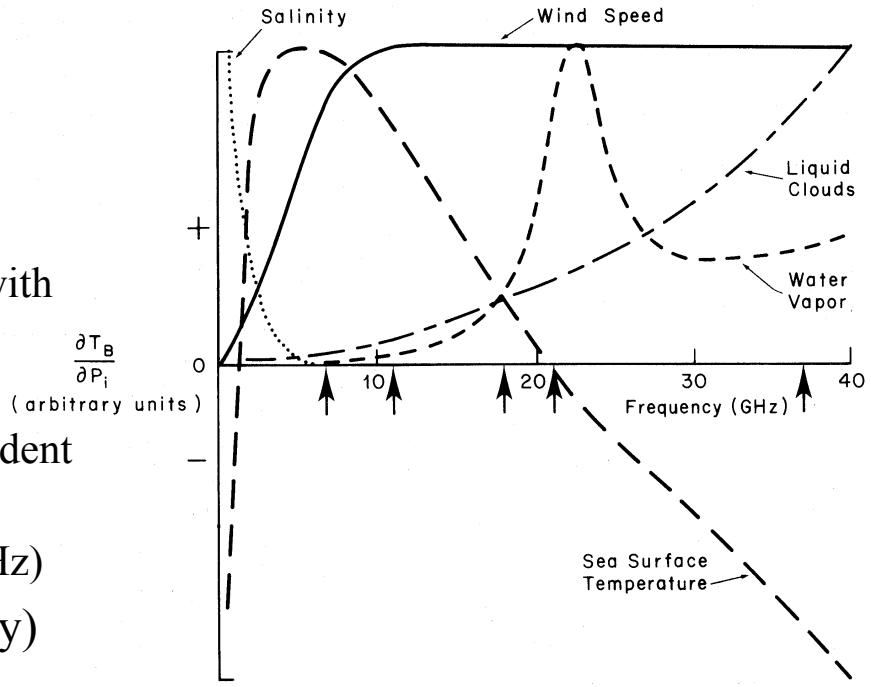

The Microwave Spectrum

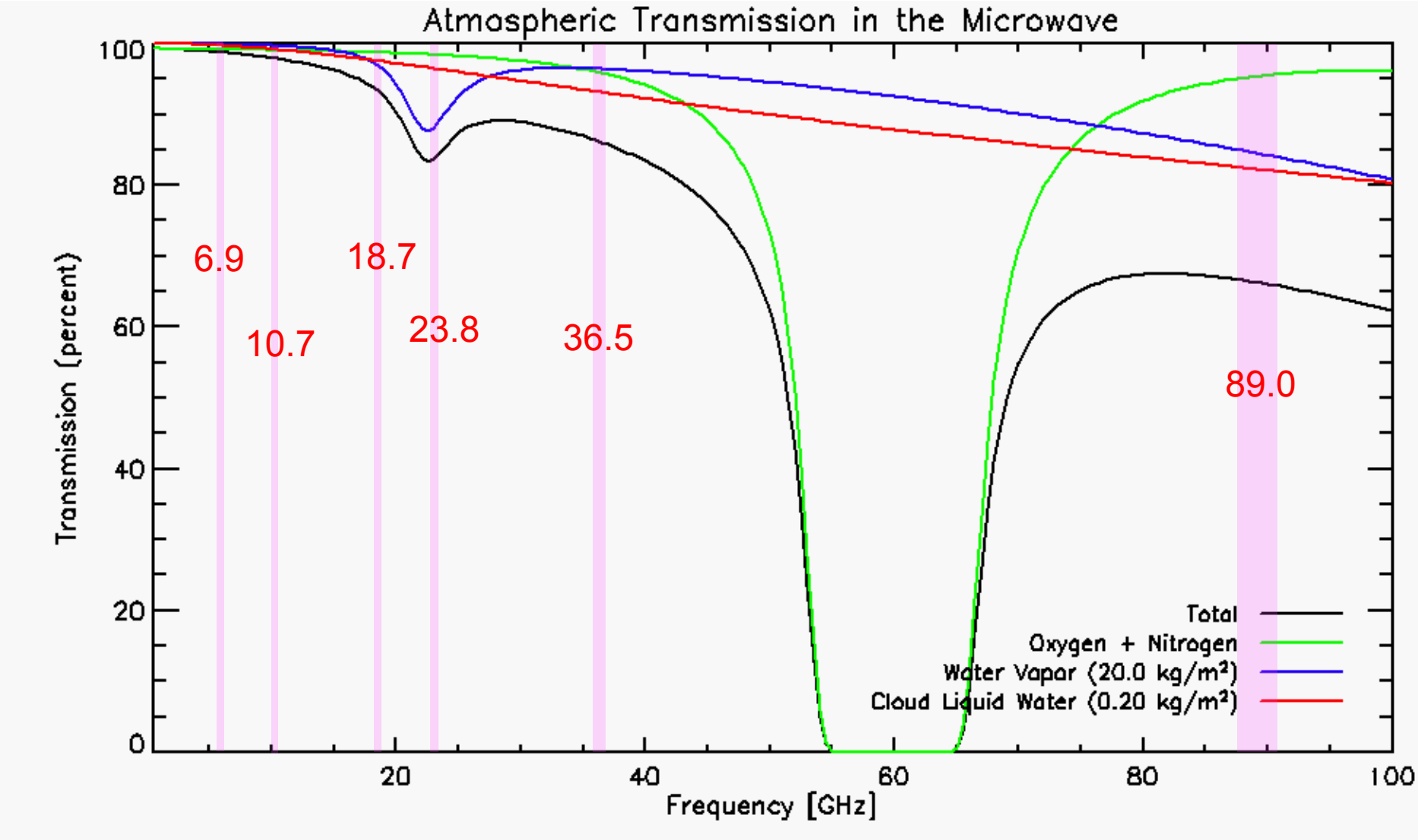

Microwave TBs depend on:

- Total column of water vapor
- Total column of cloud liquid water (+drizzle)
- Total column of rain
- Surface temperature
- Surface reflectance (depends primarily on windspeed, view angle)

Sea-Surface Emissivity (calm surface)

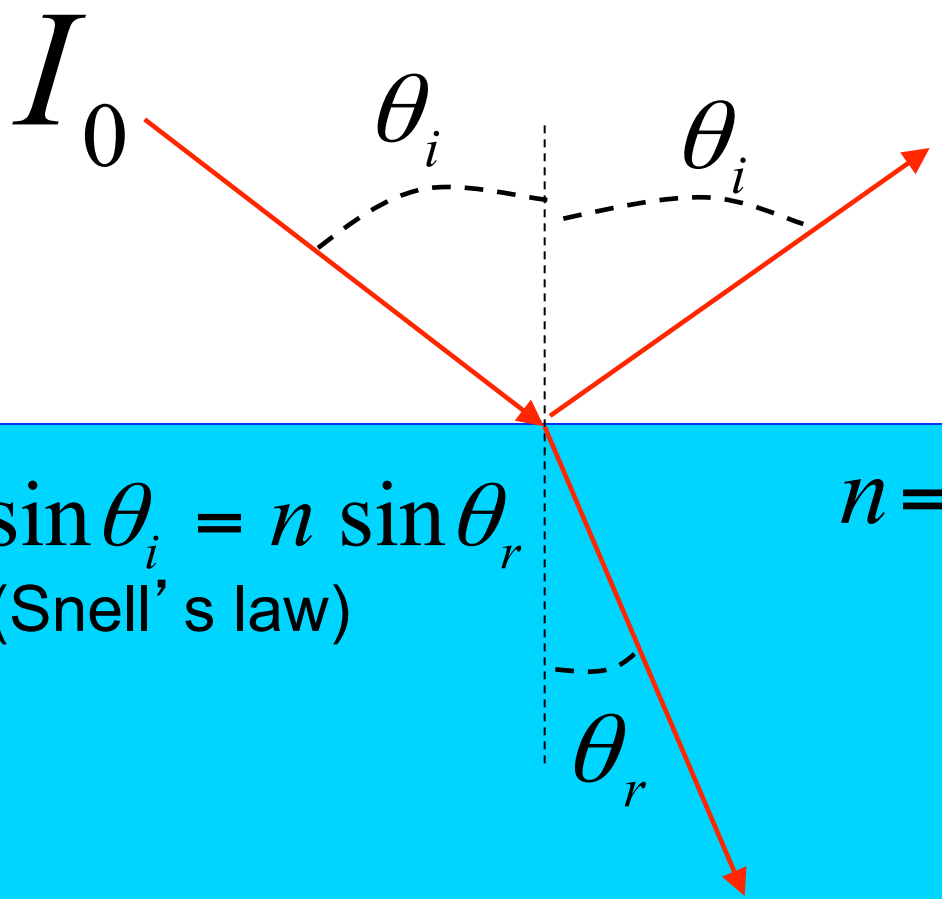

$$n_{air} \sin\theta_i = n \sin\theta_r$$

(Snell's law)

$$n = n(T, \upsilon, s) = n_r + i\, n_i$$

$$r_v = \left| \frac{\cos\theta_r - n \cos\theta_i}{\cos\theta_r + n \cos\theta_i} \right|^2$$

$$r_h = \left| \frac{\cos\theta_i - n \cos\theta_r}{\cos\theta_i + n \cos\theta_r} \right|^2$$

(Fresnel Relations)

$$\varepsilon_p = 1 - r_p$$

(Specular Assumption)

Sea-Surface Emissivity (with wind)

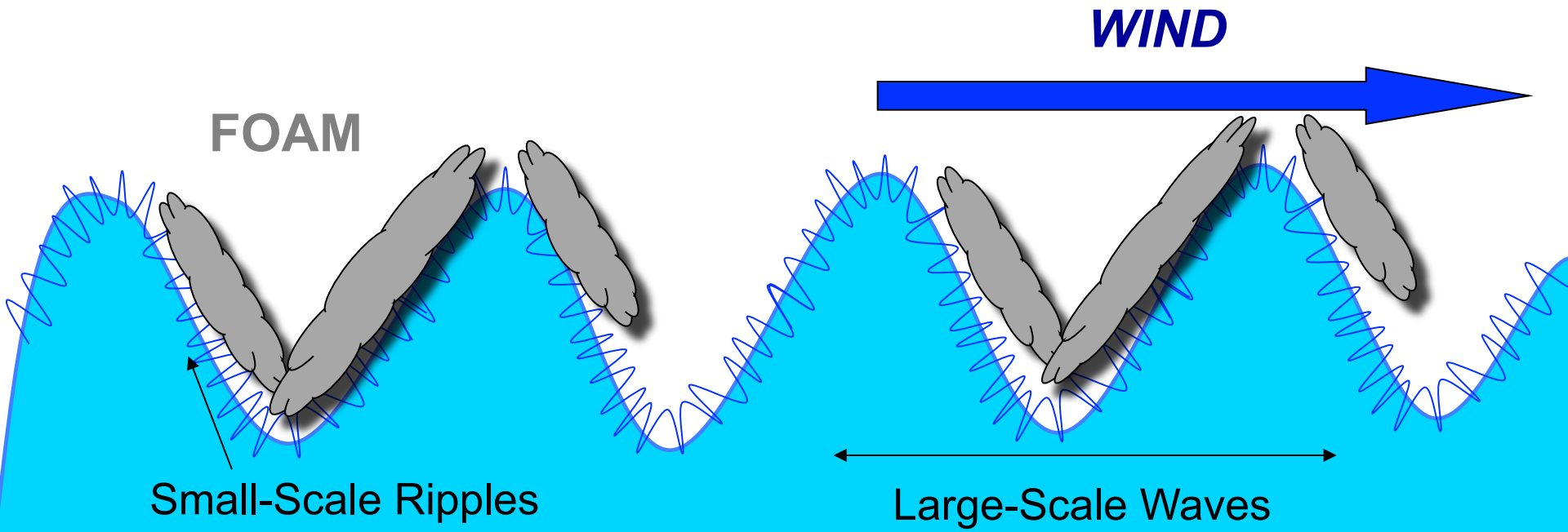

$$r_p \rightarrow B(\theta_i, \nu, W)\, r_p \qquad \text{(Ripples)}$$

$$\varepsilon_p \rightarrow \varepsilon_p + \varepsilon_p^{*}(\theta_i, \nu, W) \qquad \text{(Waves)}$$

$$\varepsilon_p \rightarrow \varepsilon_p (1 - FC) + FC \qquad \text{(Foam)}$$

$$(FC \propto W^{3.52})$$

$$r_p \rightarrow r_p \cdot \frac{1 - \tau^{\sec\theta^{*} / \sec\theta_i}}{1 - \tau}$$

(Non-Specular Correction)

Reflectance vs. Zenith Angle

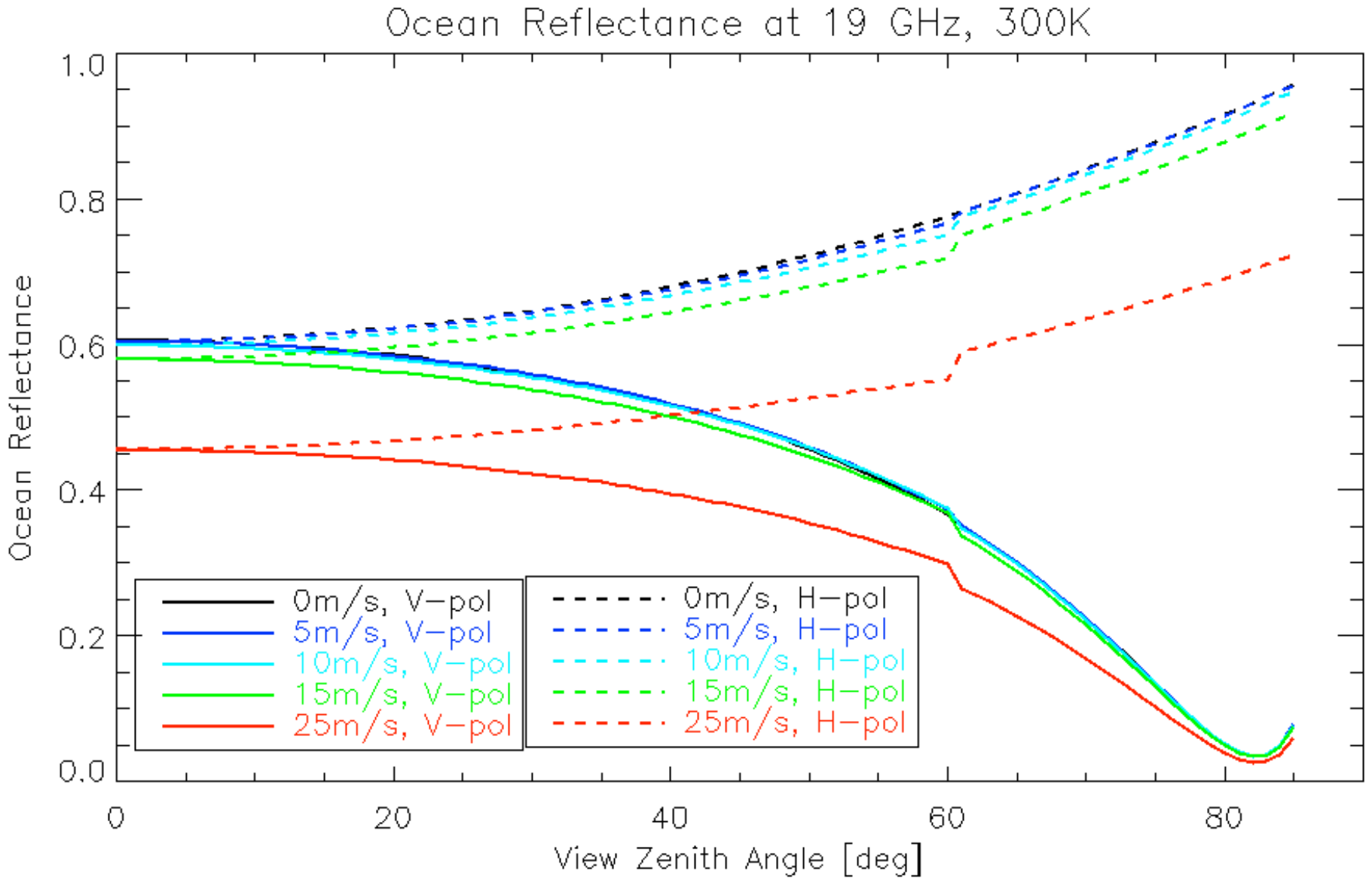

Reflectance vs. Wind Speed

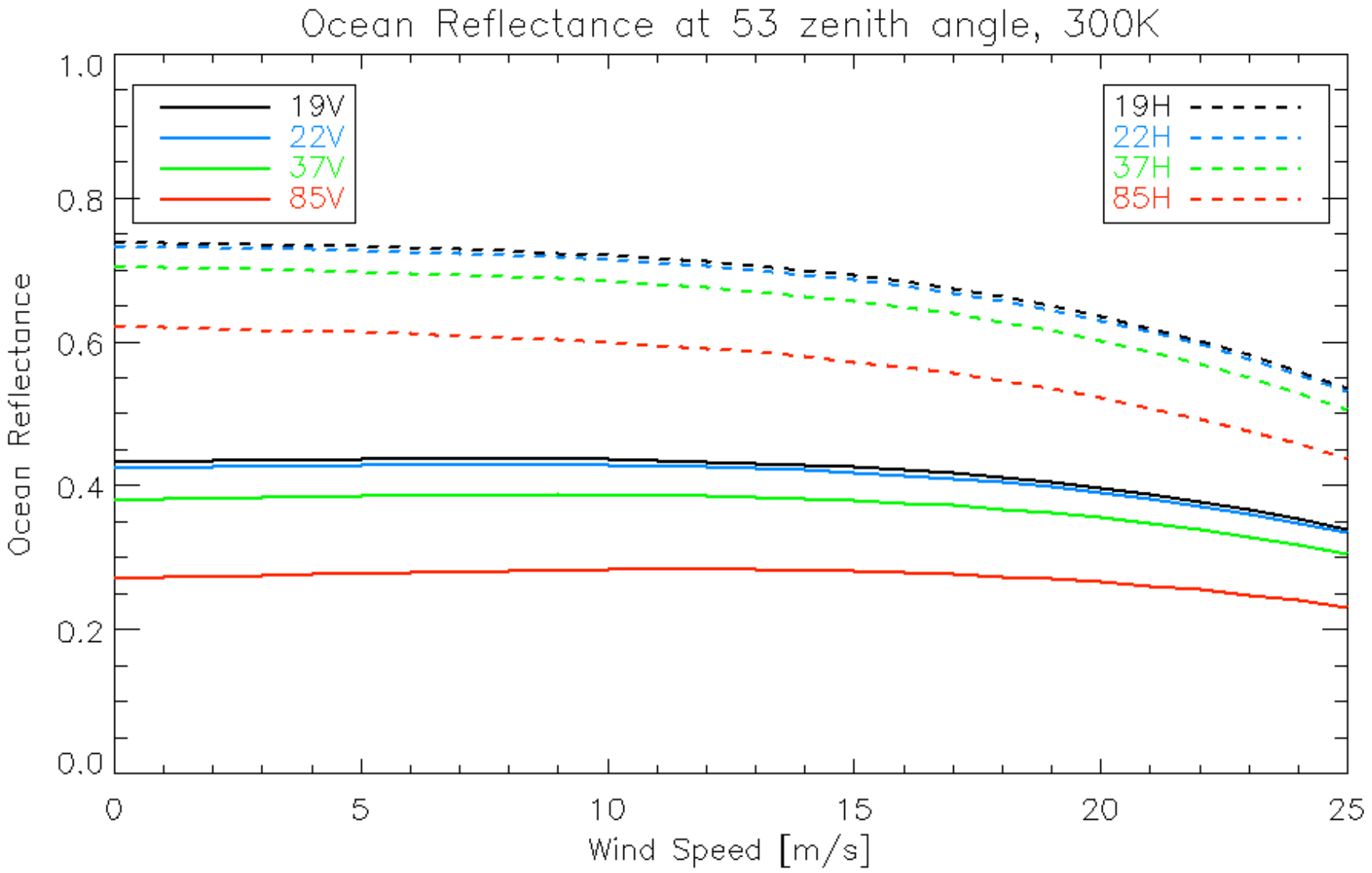

Reflectance Ratio vs. Wind Speed

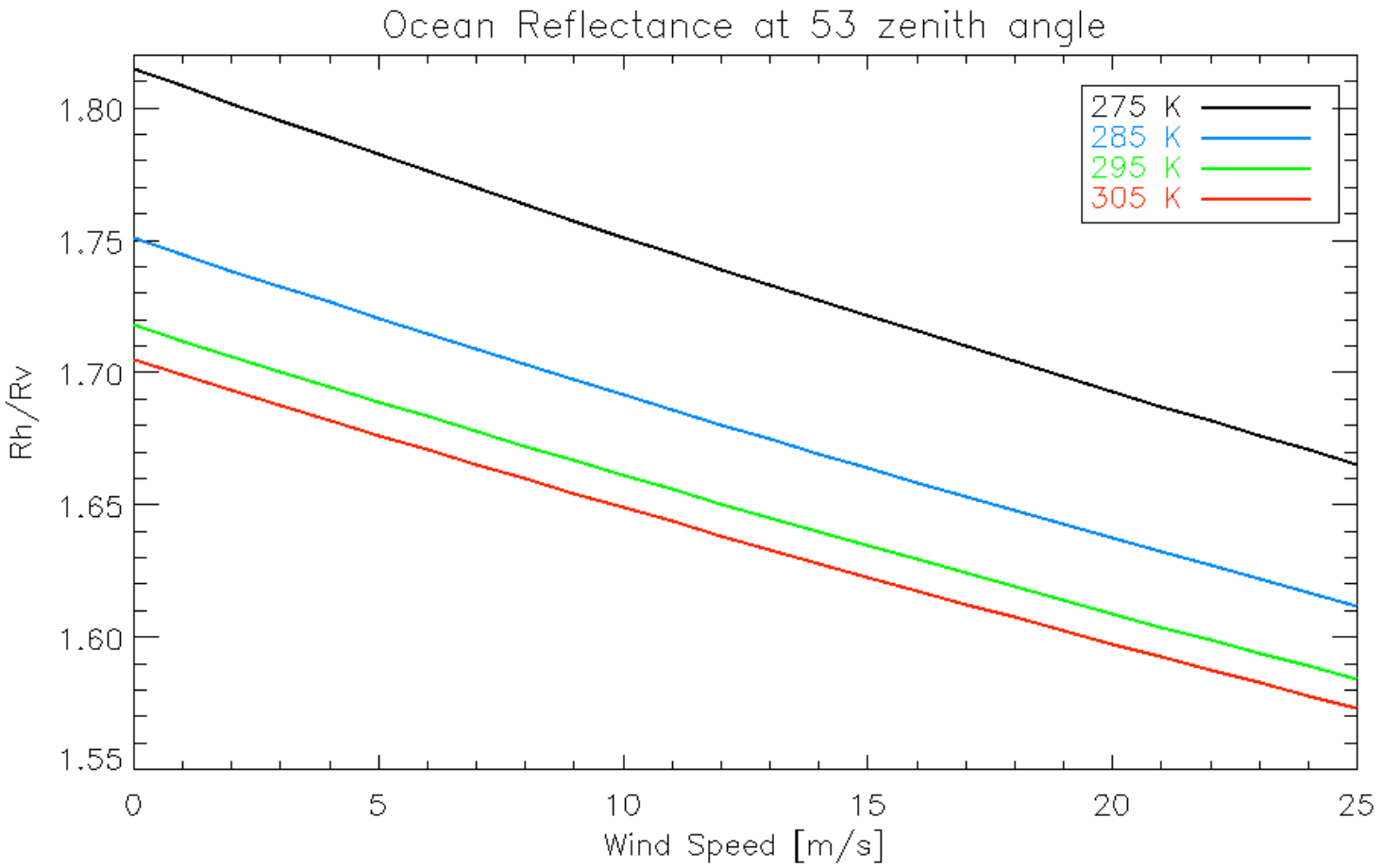

- Knowing SST, provides reasonably robust way to estimate wind speed.

Cloud water?

- Must tackle Rayleigh extinction!
- Can use the fact that cloud drops are small compared to microwave wavelengths (~1 cm)

Scattering Size Parameter

Type	Size	Number
Gas molecule	$\sim 10^{-4}$ μm	$< 3 \times 10^{19}$ cm^{-3}
Aerosol, Aitkin	< 0.1 μm	$\sim 10^{4}$ cm^{-3}
Aerosol, Large	0.1–1 μm	$\sim 10^{2}$ cm^{-3}
Aerosol, Giant	>1 μm	$\sim 10^{-1}$ cm^{-3}
Cloud droplet	5–50 μm	10^{2}–10^{3} cm^{-3}
Drizzle drop	~ 100 μm	$\sim 10^{3}$ m^{-3}
Ice crystal	10–10^{2} μm	10^{3}–10^{5} m^{-3}
Rain drop	0.1–3 mm	10–10^{3} m^{-3}
Graupel	0.1–3 mm	1–10^{2} m^{-3}
Hailstone	~ 1 cm	10^{-2}–1 m^{-3}
Insect	~ 1 cm	<1 m^{-3}
Bird	~ 10 cm	$<10^{-4}$ m^{-3}
Airplane	~ 10 m	<1 km^{-3}

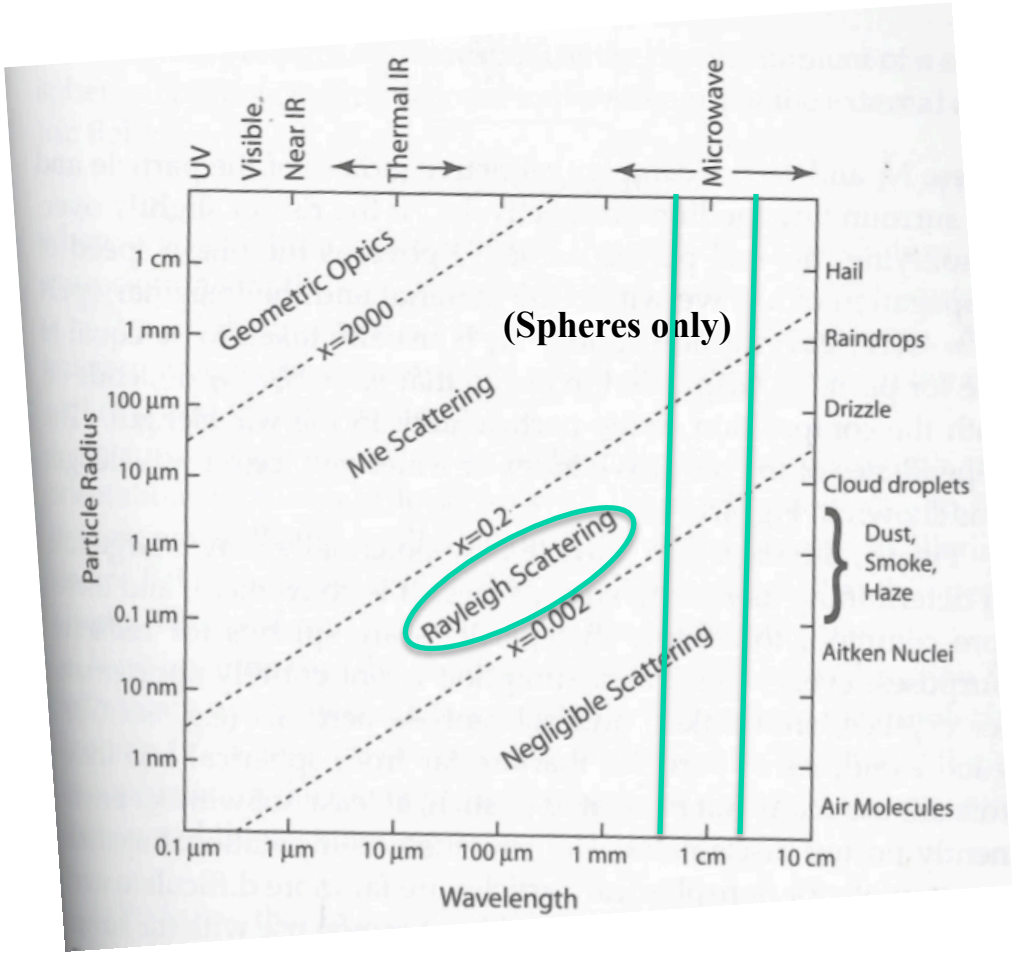

Drizzle drops and smaller are firmly in Rayleigh Regime for microwave

From Petty (2004)

Particle Extinction (single particle)

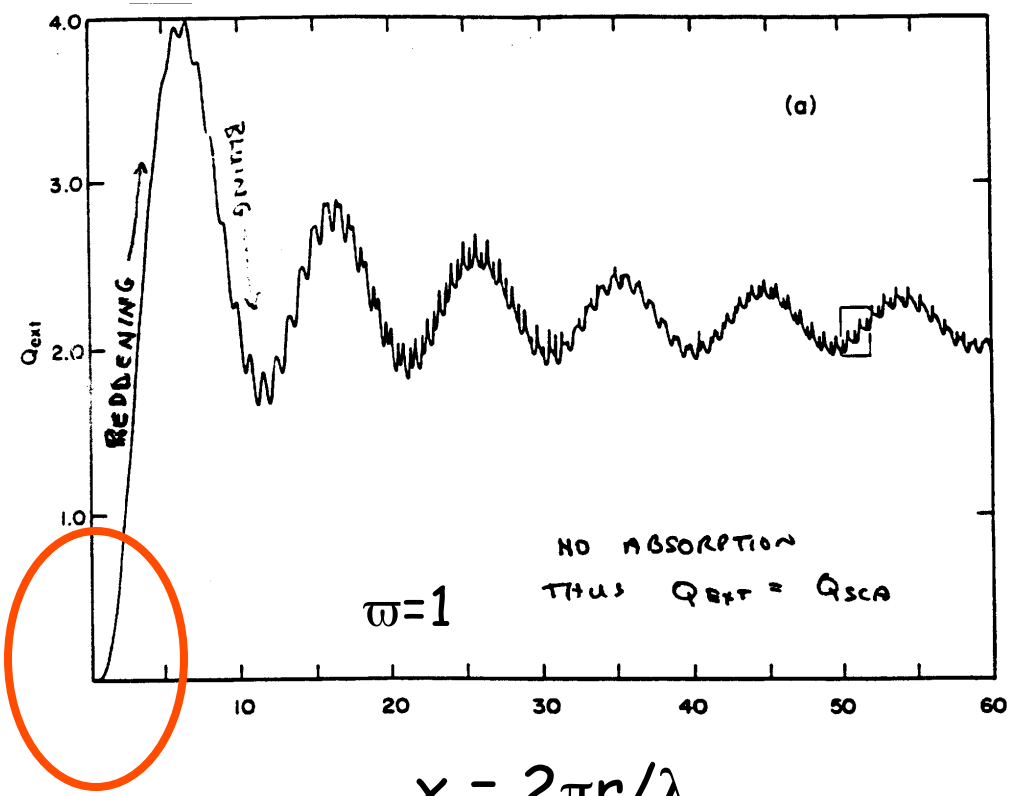

$$Q_e = \frac{\text{Extinction Cross Section}}{\text{Physical Cross Section}}$$

$x = 2\pi r/\lambda$

'Rayleigh' limit $x \rightarrow 0$ ($x \ll 1$)

Microwave (Rayleigh) scattering x→0

$$Q_{sca} \approx \frac{8}{3} x^4 \left| \frac{m^2 - 1}{m^2 + 2} \right|^2 \approx 0$$

$$Q_{abs} \approx 4x \Im m \left[\frac{m^2 - 1}{m^2 + 2} \right] \approx Q_{ext}$$

$$\mathrm{K} \equiv \frac{m^2 - 1}{m^2 + 2}$$

$$\tau = \int_{\Delta z} dz \int n(r) Q_{ext} \pi r^2 dr$$

- Cloud droplets with x<<1 for all droplets
- Optical depth τ through some depth Δz

Cloud Ice can be neglected in most microwave RT!

Volumes containing clouds of many particles

$$V = N_o \frac{4\pi}{3} r^3$$

$r \approx 10\ \mu m = 10^{-3}\ cm$

$N_0 \approx 100$ droplets per c.c

$$V \approx 100 \times \frac{4\pi}{3} \times \left(10^{-3}\right)^3$$

$V \approx 10^{-7}$

Extinctions, absorptions and scatterings by all particles simply add- volume coefficents

$$\beta_{ext,abs,sca} = \int_0^\infty n(r)\pi r^2 Q_{ext,abs,sca}(r,\lambda)dr$$

L^{-1} L^{-4} L^2 L

n(r)= the particle size distribution
particles per unit volume
per unit size

$n(r) = const\ e^{-r/a}$ Exponential distribution (rain)

$n(r) = const\ r^{\frac{1-3b}{b}} e^{-\frac{r}{ab}}$ Modified Gamma distribution (clouds)

$$n(r) = const\ \exp\left(-\frac{\left(\ln r - \ln r_0\right)^2}{2\sigma^2}\right)$$

Lognormal distribution (aerosols, sometimes clouds)

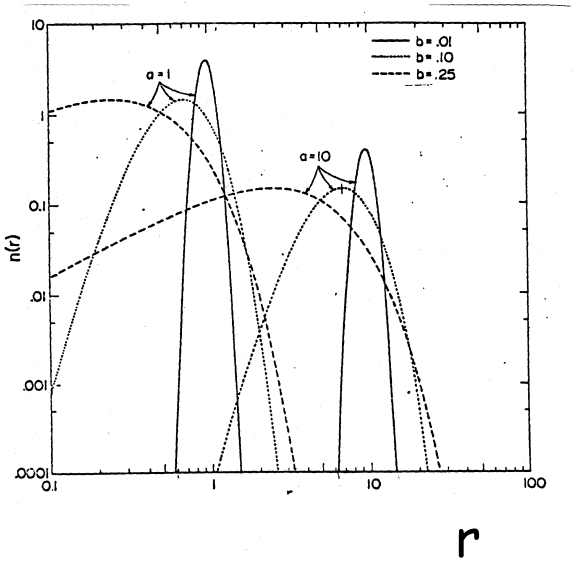

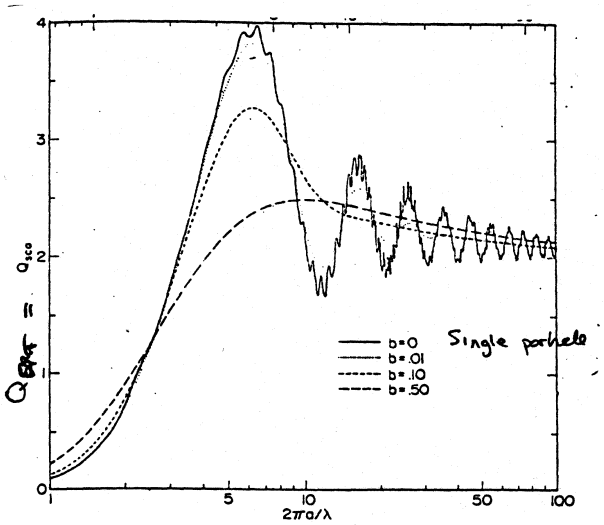

Effective Radius & Variance

$$\langle r \rangle = \frac{\int_0^\infty r\, n(r)\, dr}{\int_0^\infty n(r)\, dr}$$

Mean particle radius – doesn't have much physical relevance for radiative effects

$$r_{eff} = \frac{\int_0^\infty r\, \pi r^2\, n(r)\, dr}{\int_0^\infty \pi r^2\, n(r)\, dr}$$

For large range of particle sizes, light scattering goes like πr^2. Defines an "effective radius"

$$\nu_{eff} = \frac{\int_0^\infty (r - r_{eff})^2\, \pi r^2\, n(r)\, dr}{r_{eff}^2 \int_0^\infty \pi r^2\, n(r)\, dr}$$

"Effective variance"

$n(r) = const\ \mathrm{r}^{\frac{1-3b}{b}}\, e^{-\frac{r}{ab}}$ Modified Gamma distribution

a = effective radius

b = effective variance

Effective Radius & Variance

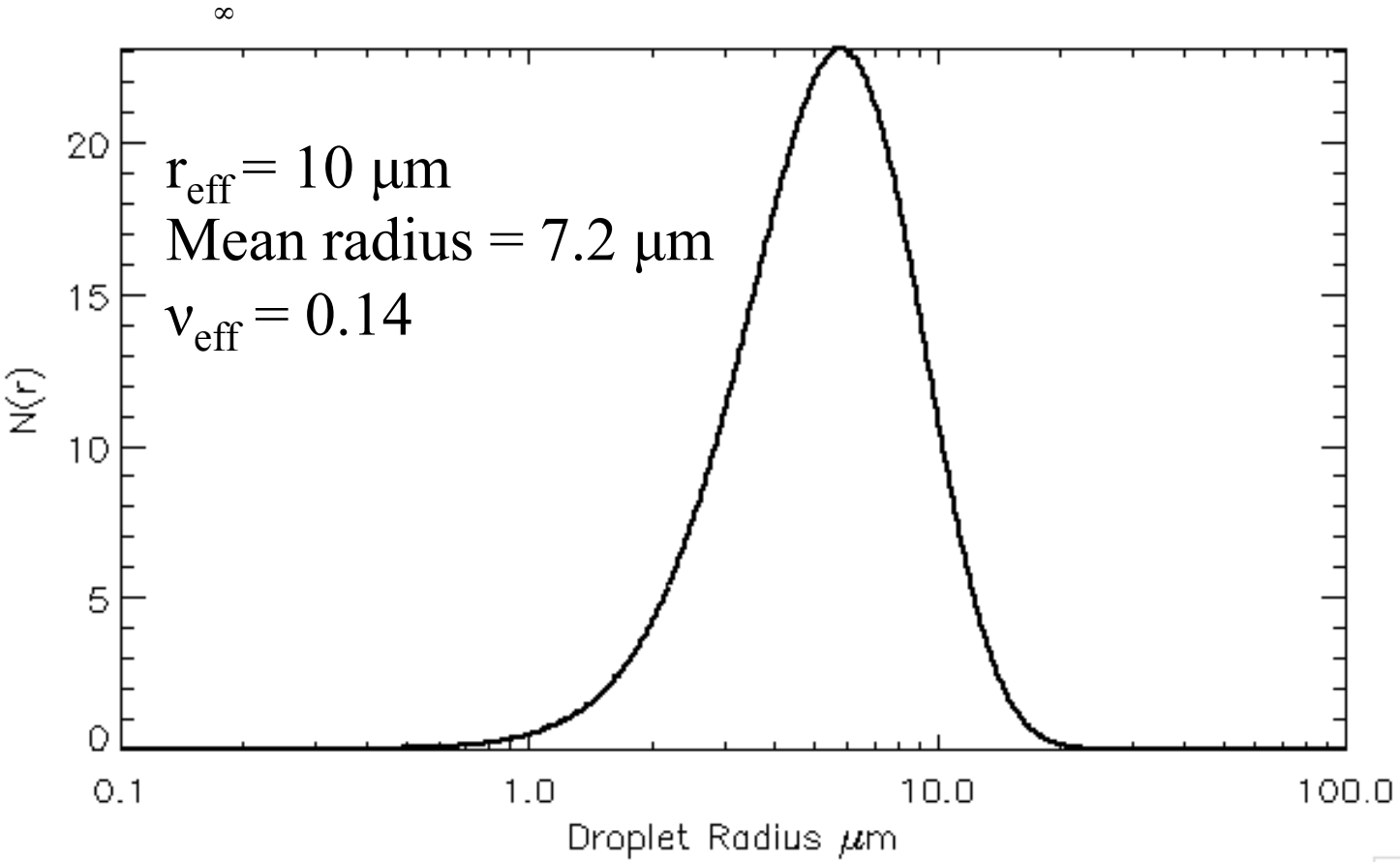

nuch
:s

scattering
dius"

$$n(r) = const\ r^{\frac{1-3b}{b}} e^{-\frac{r}{ab}}$$ Modified Gamma distribution

a = effective radius
b = effective variance

Microwave (Rayleigh) scattering x→0

$$Q_{sca} \approx \frac{8}{3} x^4 \left| \frac{m^2 - 1}{m^2 + 2} \right|^2 \approx 0$$

$$Q_{abs} \approx 4x \Im m\left[\frac{m^2 - 1}{m^2 + 2} \right] \approx Q_{ext}$$

$$\mathrm{K} \equiv \frac{m^2 - 1}{m^2 + 2}$$

$$\tau = \int_{\Delta z} dz \int n(r) Q_{ext} \pi r^2 dr$$

$$\approx \frac{8\pi}{\lambda} \Im m(\mathrm{K}) \int_{\Delta z} dz \int n(r) \pi r^3 dr$$

$$L = \frac{4\pi\rho}{3} \int \int n(r) r^3 dr\, dz$$

$$\tau \approx \frac{6\pi}{\lambda\rho} \Im m(\mathrm{K})\, \mathrm{L}$$

Distribution of water cloud drops can be completely ignored in microwave

- Cloud droplets with x<<1 for all droplets
- Optical depth τ through some depth Δz
- τ depends only on total water path L, the index of refraction of water or ice (through K), and the density of water/ice.

Ex: 37 GHz, 0.5 kg/m^2
Water: K ~ 0.11 ; Ice K ~ 3.1e-4
τ_{wat}~ 0.13 ; τ_{ice}~ 4e-4

Cloud Ice can be neglected in most microwave RT!

Retrieving path integrated water vapor and cloud liquid water from microwave radiances

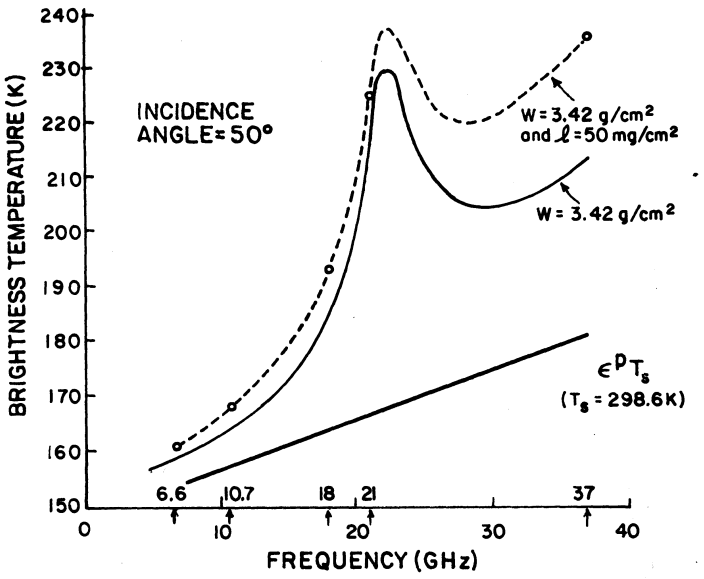

Microwave spectrum around the 22 GHZ water vapor absorption line

$$\left(e^{-\tau^*/\mu}\right)_w \sim e^{-k_w w}$$

$$\left(e^{-\tau^*/\mu}\right)_\ell \sim e^{-k_\ell W}$$

$$k_\ell L + k_w W = \frac{\mu}{2}\ln\frac{\Delta T}{T_S(R_V - R_H)Tr_{ox}^2}$$

(*i*) *Emission from the atmosphere*

$$\int_0^{\tau^*} B_\lambda(t)\, e^{-t/\mu}\frac{dt}{\mu} \sim T_S(1-e^{-\tau^*/\mu})$$

(ii) Emission from the surface

$$(1-R_{V,H})e^{-\tau^*/\mu}T_S$$

(*iii*) Atmospheric emission - surface reflection

$$R_{V,H}e^{-\tau^*/\mu}\int_{\tau^*}^{0} B_\lambda(t)\, e^{-t/\mu}\frac{dt}{\mu} \sim R_{V,H}e^{-\tau^*/\mu}(1-e^{-\tau^*/\mu})T_S$$

Total brightness temperature

$$T_{V,H} = (1-R_{V,H})e^{-\tau^*/\mu}T_S + R_{V,H}e^{-\tau^*/\mu}(1-e^{-\tau^*/\mu})T_S + T_S(1-e^{-\tau^*/\mu})$$

$$T_{V,H} = T_S[1-\left(e^{-\tau^*/\mu}\right)^2 R_{V,H}]$$

$$\Delta T = T_H - T_V = T_S(R_V - R_H)\left(e^{-\tau^*/\mu}\right)^2$$

$$\left(e^{-\tau^*/\mu}\right)^2 = Tr_w^2 Tr_W^2 Tr_{ox}^2$$

Simple Wind Parameterization

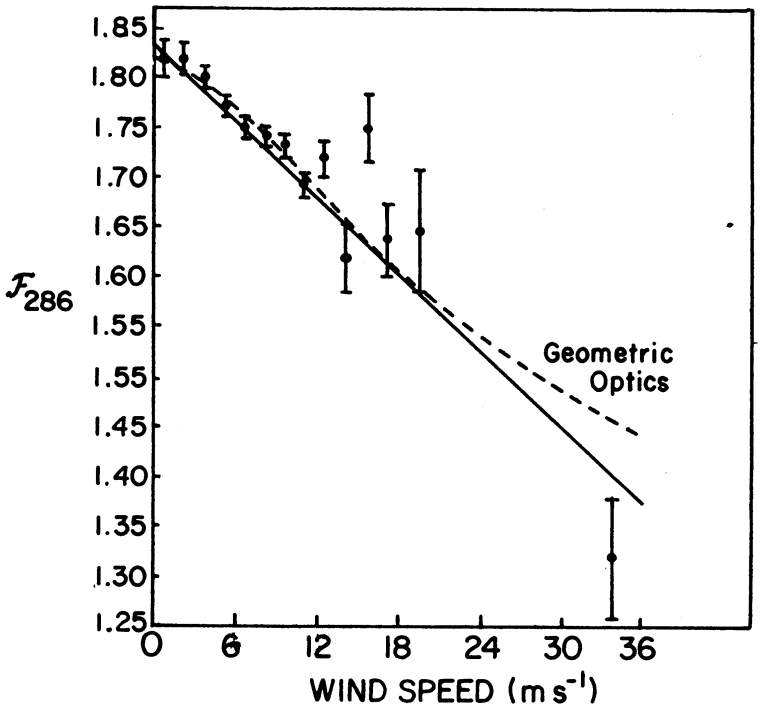

$$T_{l,r} = (1 - R_{l,r})e^{-\tau^*/\mu}T_{ocean} + R_{l,r}e^{-\tau^*/\mu}T_{sky} + T_{sky}$$

Consider; $e^{-\tau^*/\mu} \sim 1$, lower frequencies

$$R_{l,r}(T_{sky} - T_{ocean}) = T_{l,r} - T_{ocean}$$

$$F = \frac{T_r - T_{ocean}}{T_l - T_{ocean}} = \frac{R_r}{R_l}$$

Measurement of $T_{l/r}$ (preferably near Brewster's angle) and *a priori* knowledge of SST yields the ratio of reflectances and thus wind speed.

Greenwald & Stephens (1993)

Measurement of ΔT at two frequencies (19GHz, 37 GHz), estimation of $R_{V/H+}$ $\Delta k_{w/l}$, and Tr_{ox} allows for simultaneous solution for W and L,

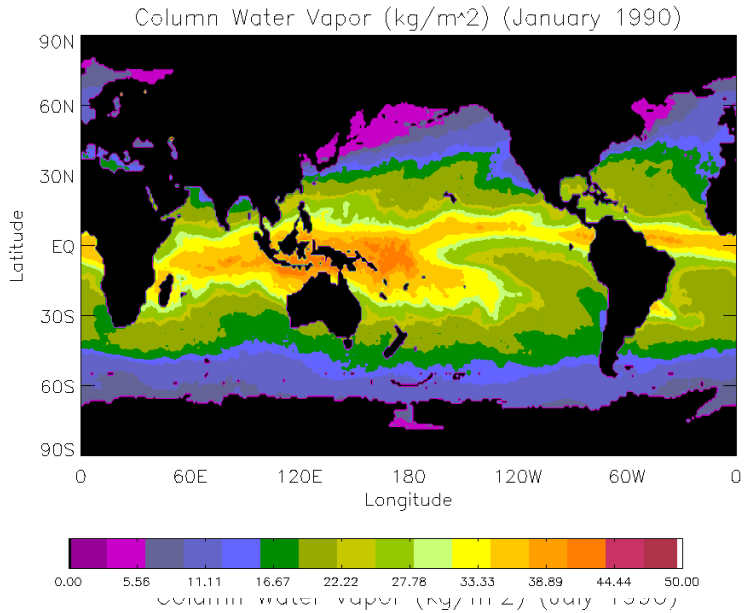

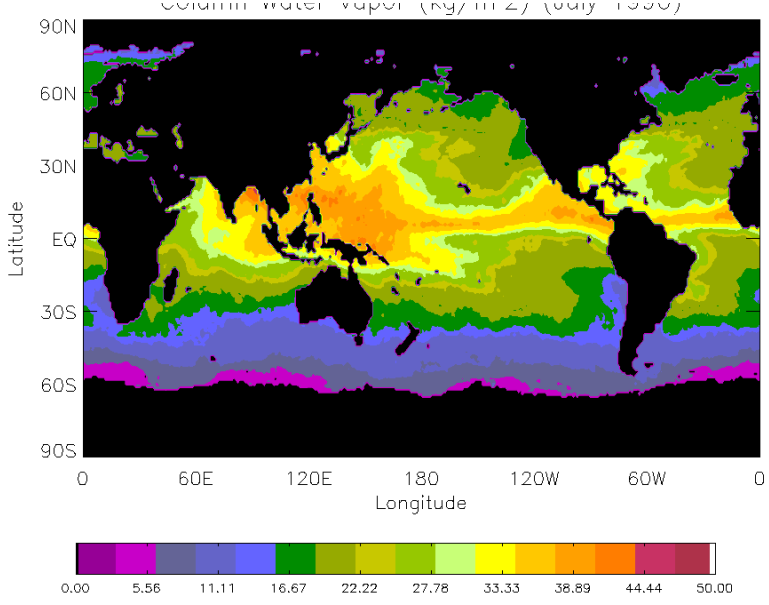

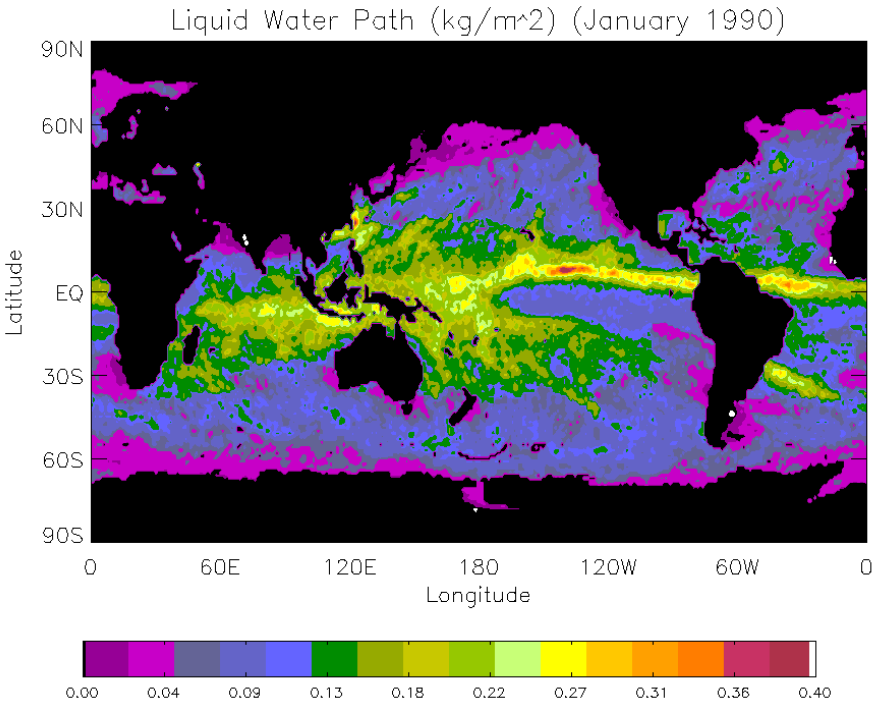

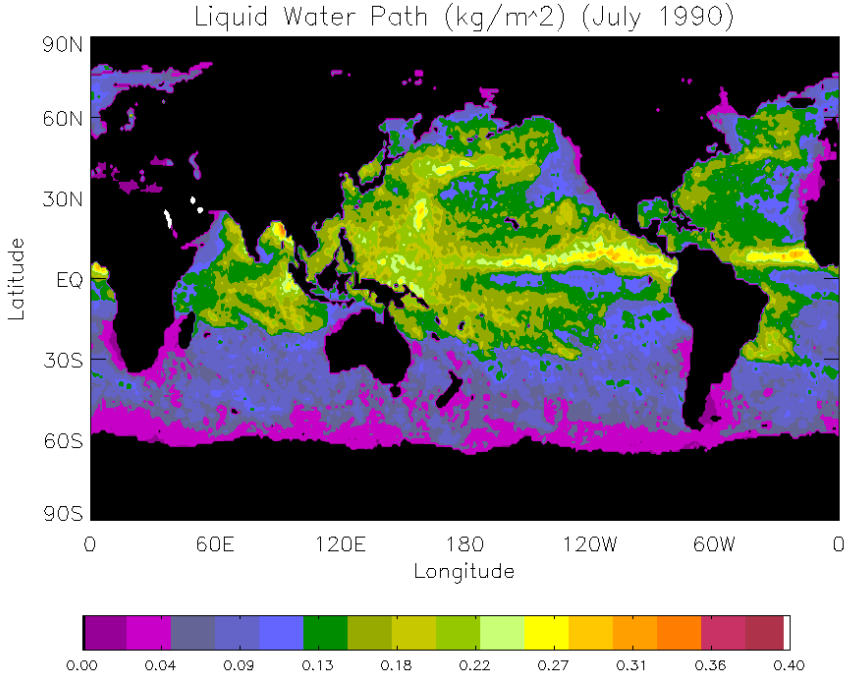

A Well Calibrated Ocean Algorithm for SSM/I

Frank J. Wentz
Remote Sensing Systems
Santa Rosa, CA 95404
wentz@indy.remss.com

Abstract

We describe an algorithm for retrieving geophysical parameters over the ocean from SSM/I observations. This algorithm is based on a model for the brightness temperature (T_B) of the ocean and intervening atmosphere. The retrieved parameters are the near-surface wind speed W, the columnar water vapor V, the columnar cloud liquid water L, and the line-of-sight wind W_{LS}. We restrict our analysis to ocean scenes free of rain, and when the algorithm detects rain, the retrievals are discarded. The model and algorithm are precisely calibrated using a very large *in situ* data base containing 37,650 SSM/I overpasses of buoys and 35,108 overpasses of radiosonde sites. A detailed error analysis indicates that the T_B model rms accuracy is between 0.5 and 1 K and that the rms retrieval accuracies for wind, vapor, and cloud are 0.9 m/s, 1.2 mm, and 0.025 mm, respectively. The error in specifying the cloud temperature will introduce an additional 10% error in the cloud water retrieval. The spatial resolution for these accuracies is 50 km. The systematic errors in the retrievals are smaller than the rms errors, being about 0.3 m/s, 0.6 mm, and 0.005 mm for W, V, and L. The one exception is the systematic error in wind speed of - 1.0 m/s that occurs for observations within $\pm 20^\circ$ of upwind. The inclusion of the line-of-sight wind W_{LS} in the retrieval significantly reduces the error in wind speed due to wind direction variations. The wind error for upwind observations is reduced from - 3.0 m/s to - 1.0 m/s. Finally, we find a small signal in the 19 GHz, h-pol T_B residual ΔT_{BH} that is related to the effective air pressure of the water vapor profile. This information may be of some use in specifying the vertical distribution of water vapor.

SSM/I Physical Retrieval Methodology

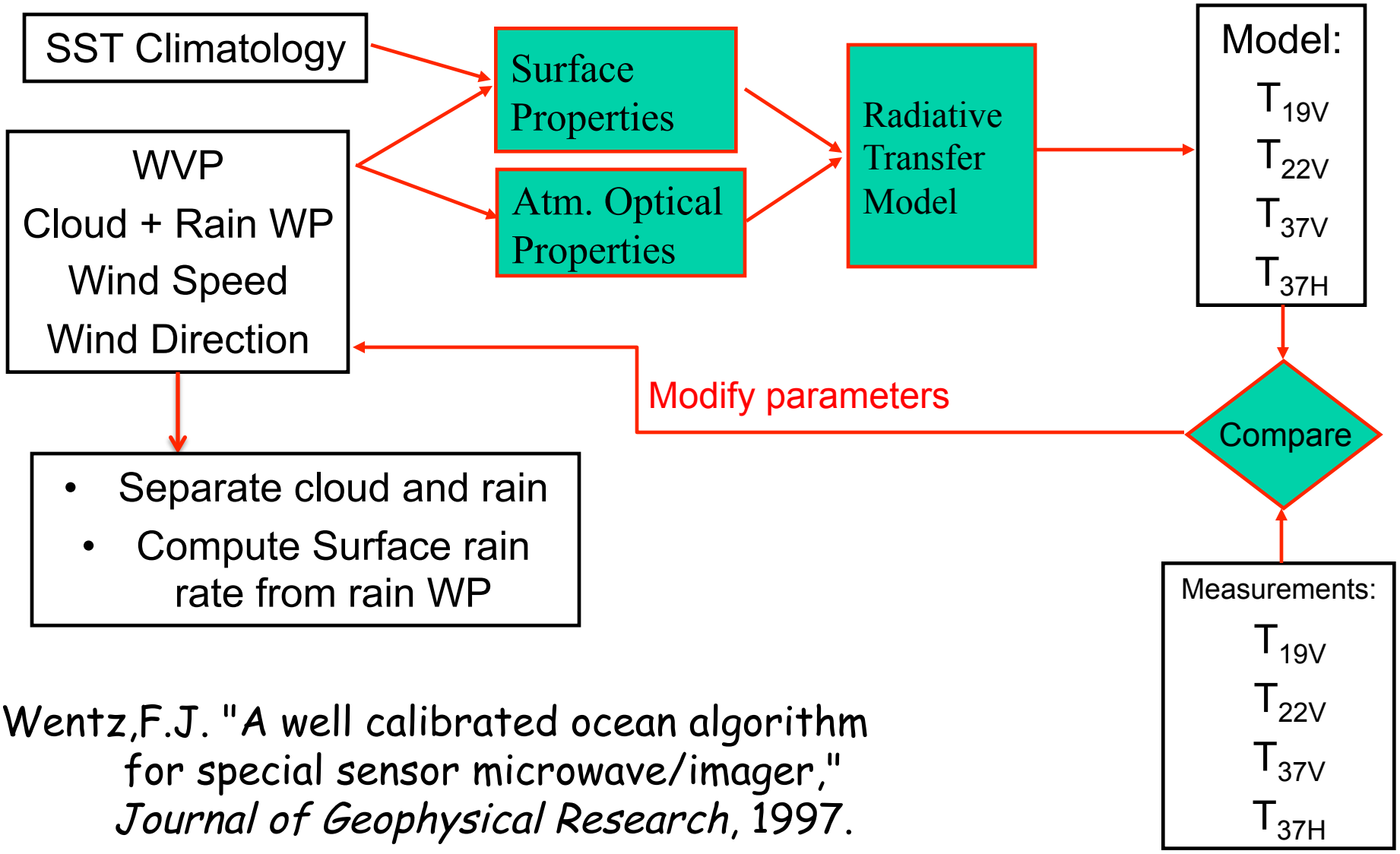

Wentz,F.J. "A well calibrated ocean algorithm for special sensor microwave/imager," *Journal of Geophysical Research*, 1997.

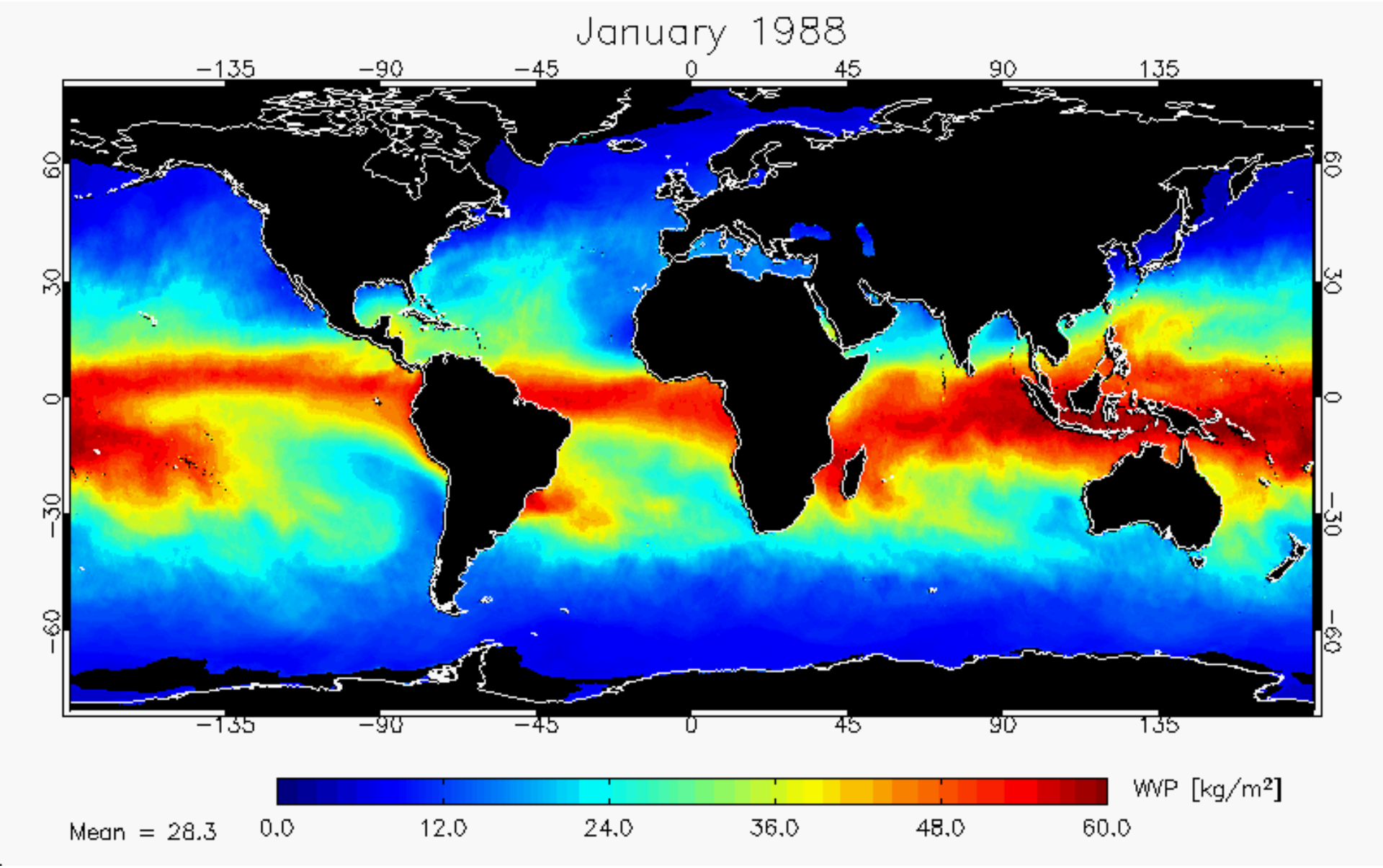
January 1988
−135
−90
−45
0
45
90
135
60
30
0
−30
−60
WVP [kg/m²]
Mean = 28.3
0.0
12.0
24.0
36.0
48.0
60.0

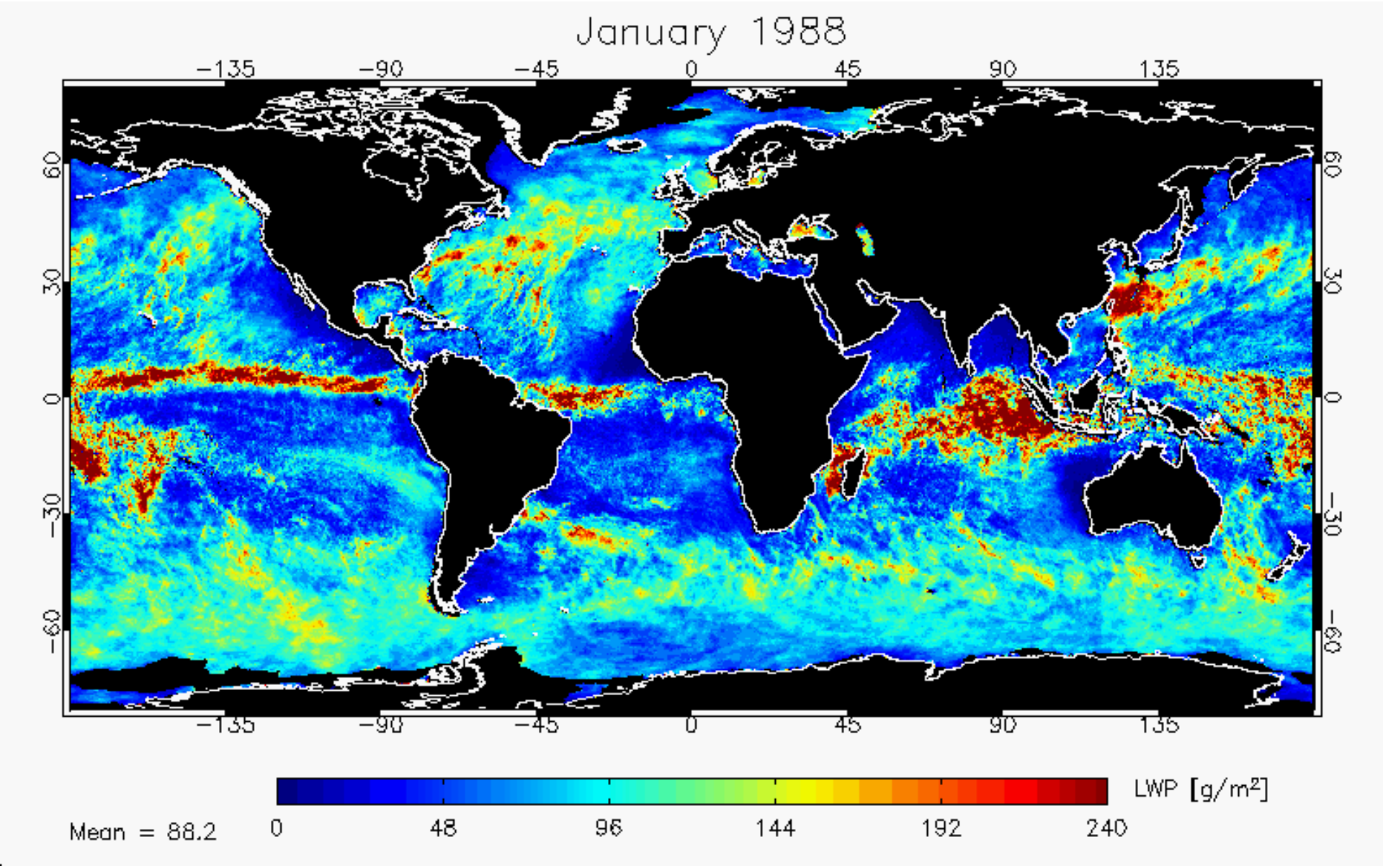
January 1988
−135
−90
−45
0
45
90
135
60
30
0
−30
−60
LWP [g/m²]
Mean = 88.2
0
48
96
144
192
240

Increase of Water Vapor over time

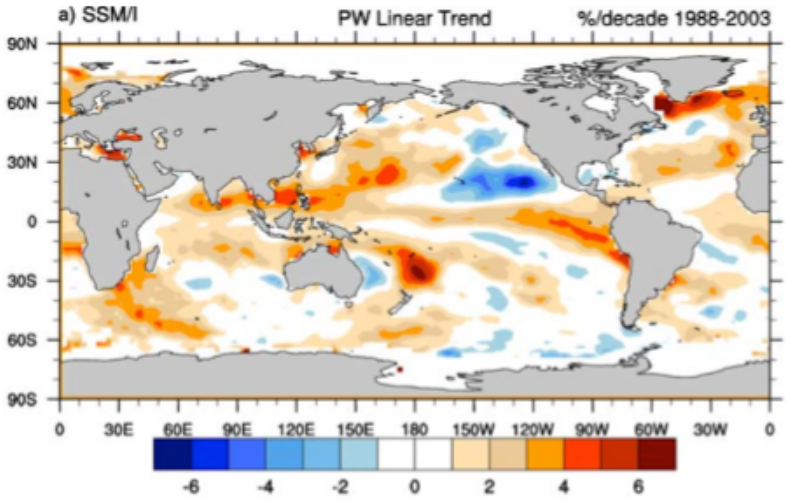

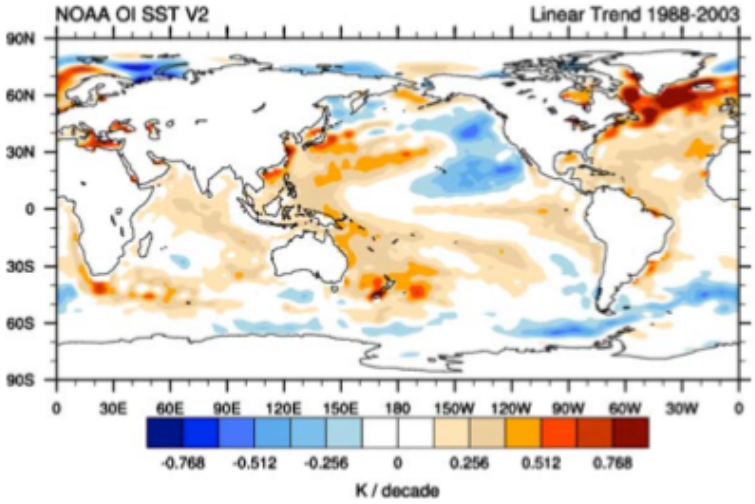

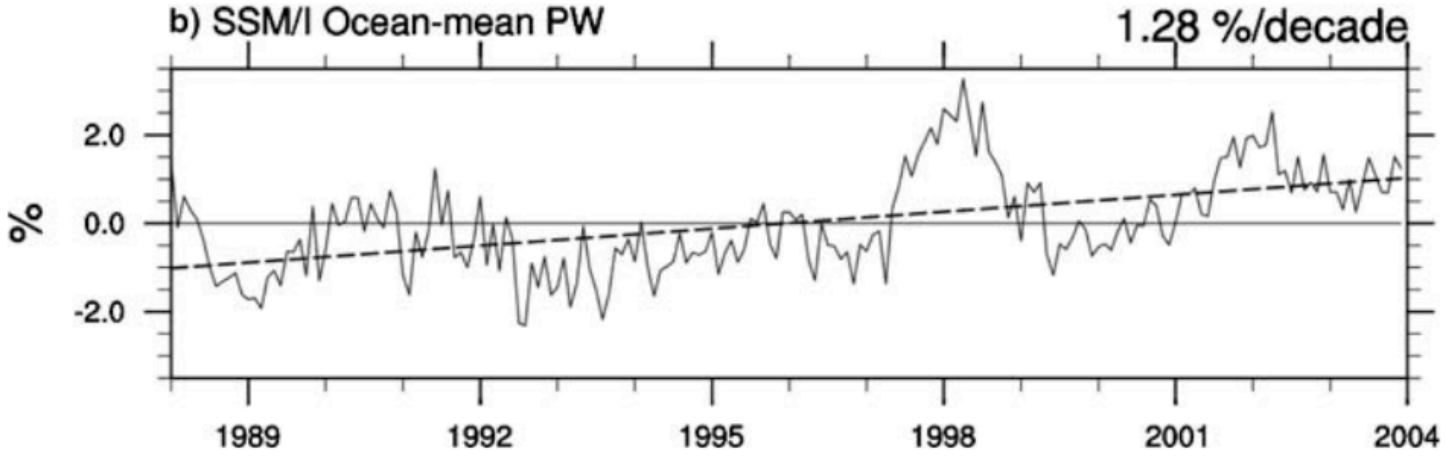

Trenberth et al. (2005)

~20 yrs Cloud Water from Multiple Satellites

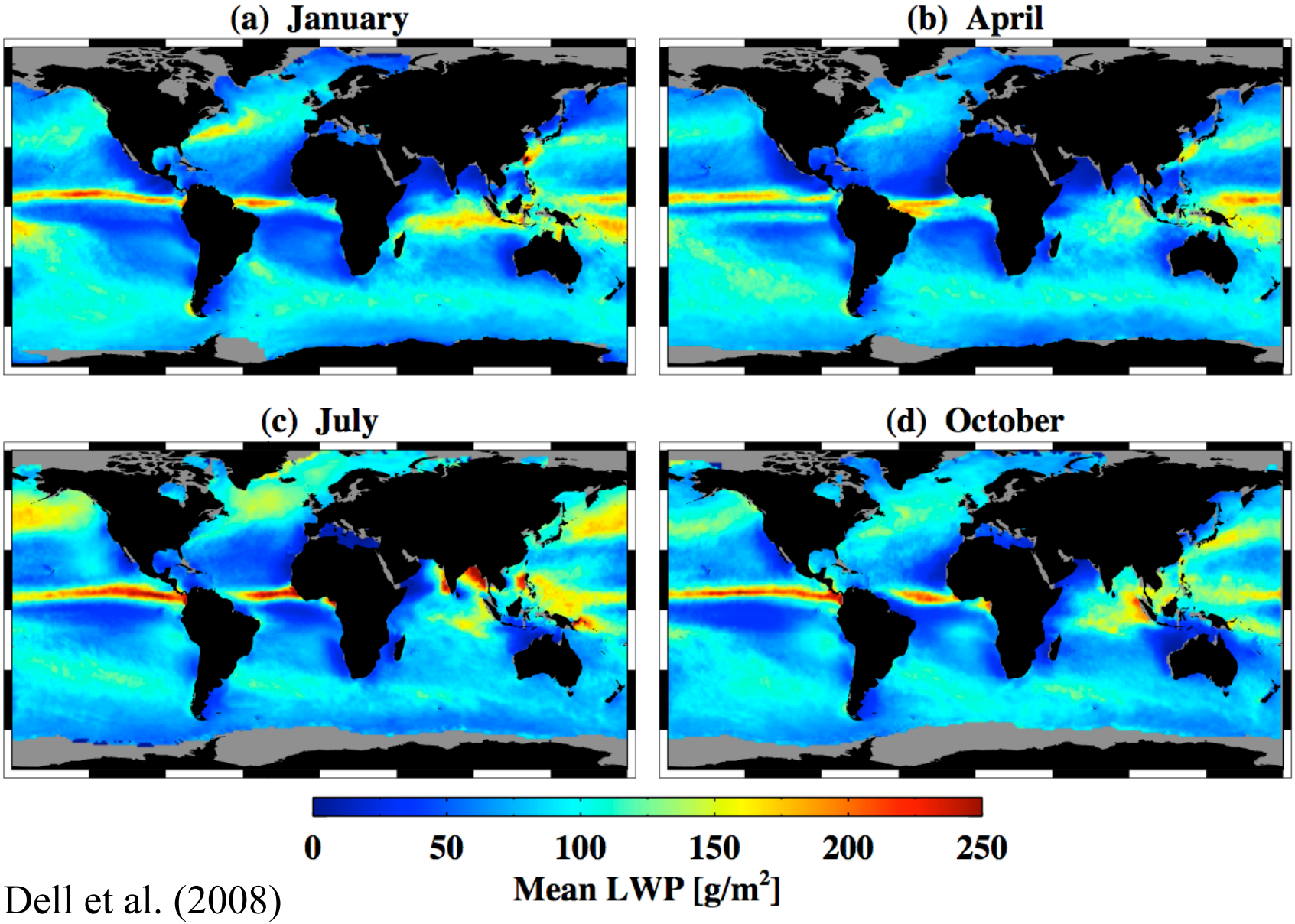

O'Dell et al. (2008)

Diurnal cycle of Cloud Water from Multiple Satellites

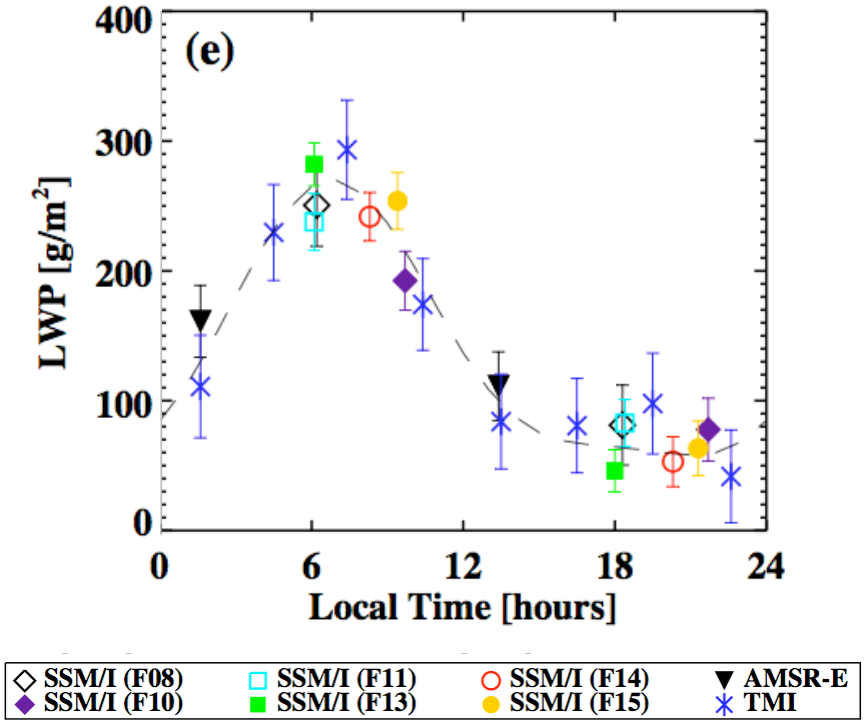

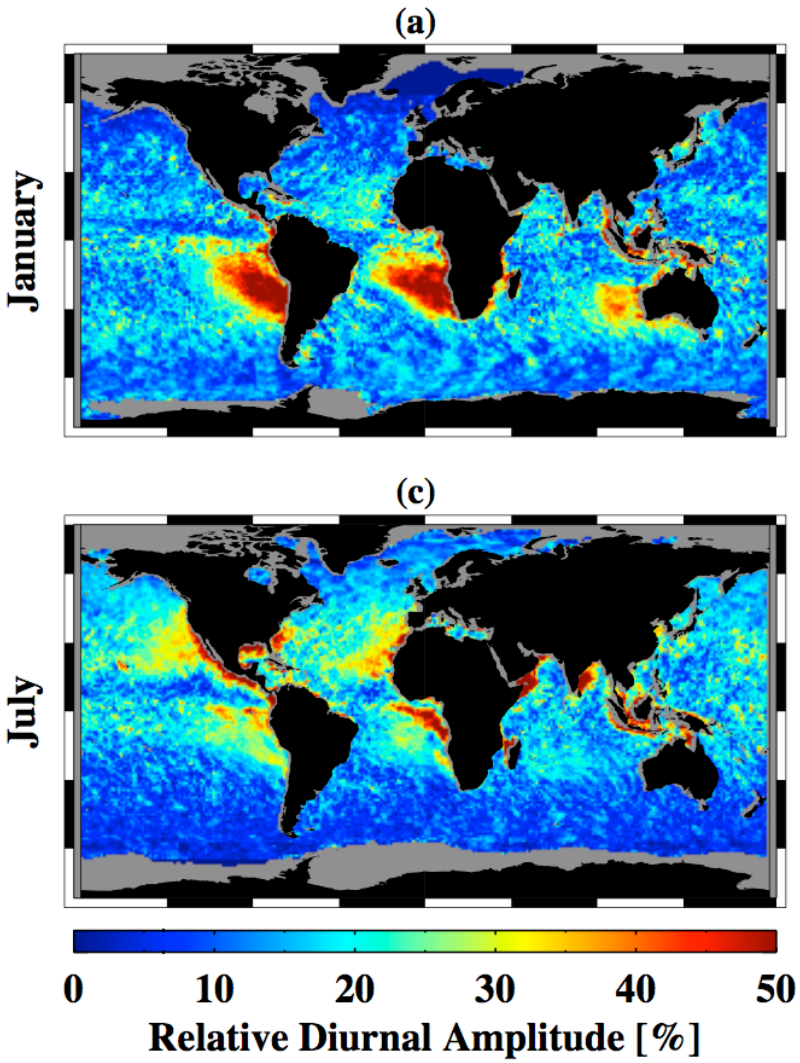

Wood et al. (2002)
O'Dell et al. (2008)

SSM/I Water Vapor & Cloud Liquid Water

October 27, 1999

Precipitable Water Vapor (mm)

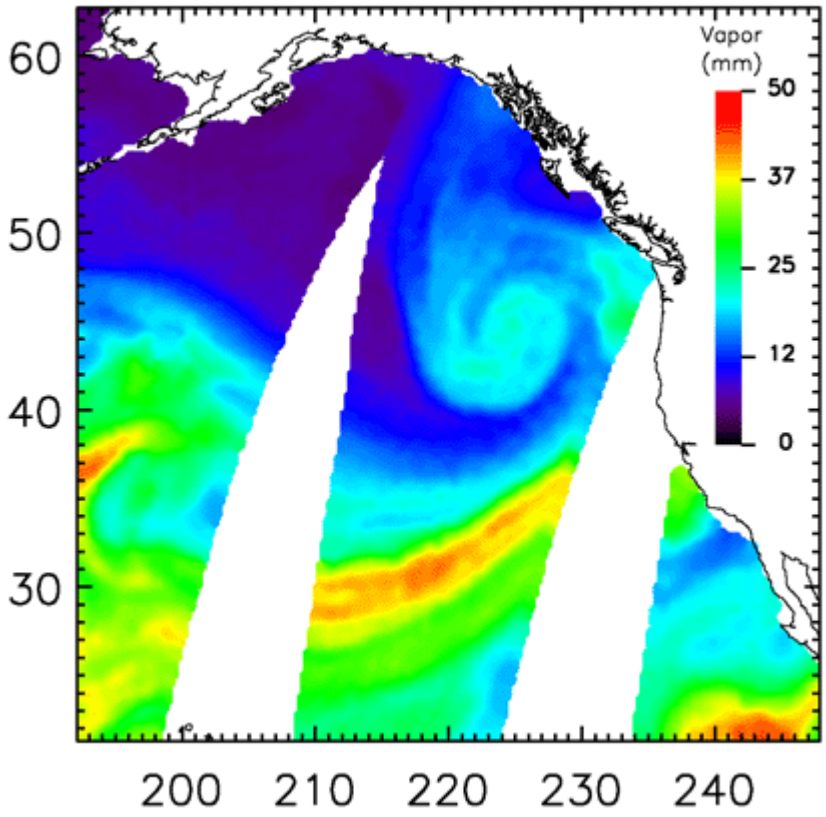

Cloud Liquid Water Path (mm)

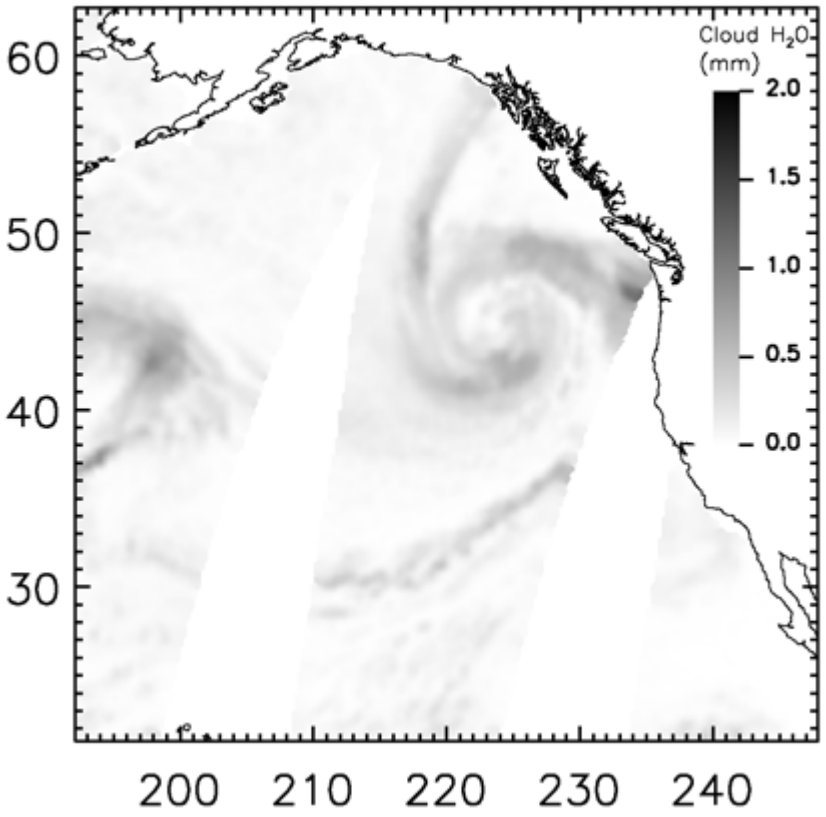

SSM/I Wind Speed & Rainfall Rate

October 27, 1999

Wind Speed (m/s)

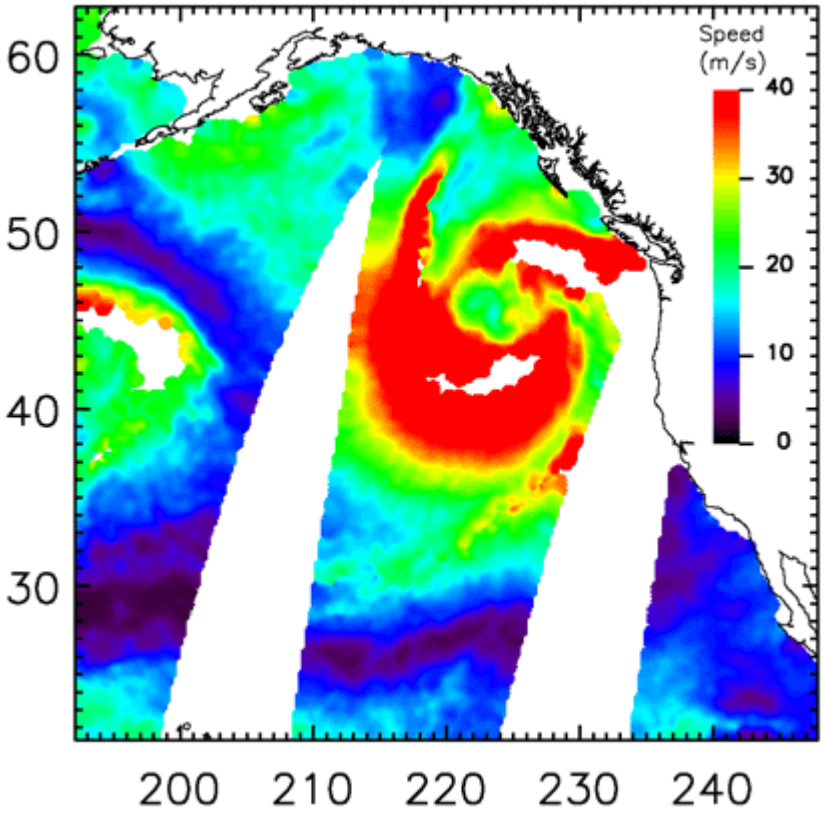

Rain Rate (mm/hr)

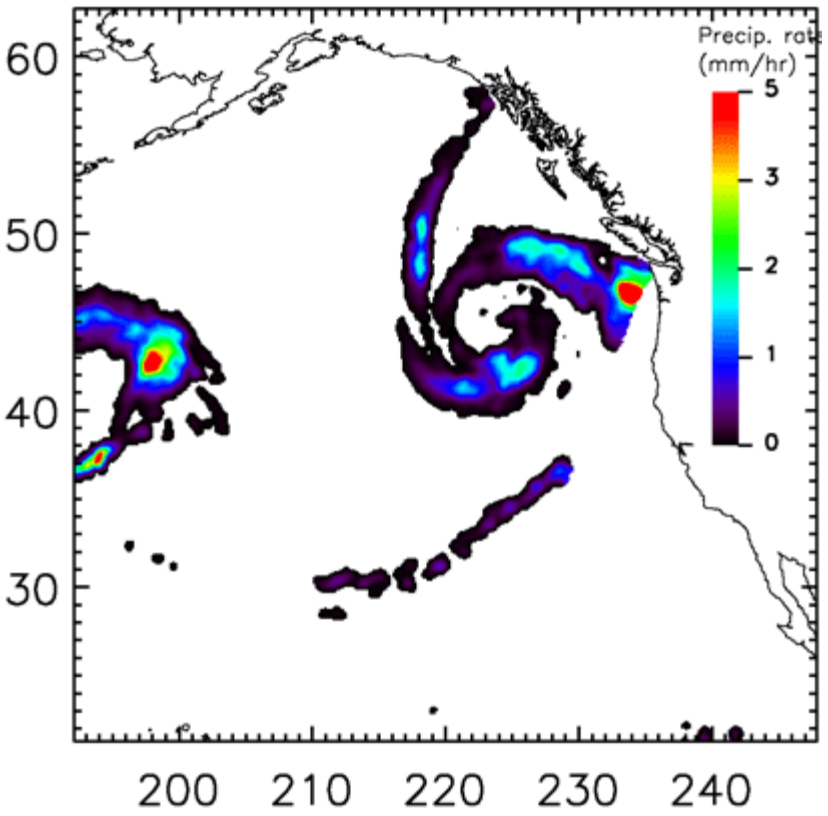

GPM Mission Concept

Unify and advance precipitation measurements from space to provide next-generation global precipitation products within a consistent framework

Low Inclination Observatory (40°)

GPM Core Observatory (65°)

- Enhanced capability for near realtime monitoring of hurricanes & midlatitude storms
- Improved estimation of rainfall accumulation

- Precipitation physics observatory
- Transfer standard for inter-satellite calibration of constellation sensors

Partner Satellites:

MetOp, NOAA-19

NPP, JPSS (over land)

Coverage & Sampling

- 1-2 hr revisit time over land
- < 3 hr mean revisit time over 90% of globe

Key Advancement

Using an advanced radar/radiometer measurement system to improve constellation sensor retrievals

Fig. from Arthur Hou

Core Observatory Measurement Capabilities

Dual-Frequency (Ku-Ka band) Precipitation Radar (DPR):

- *Increased sensitivity (~12 dBZ) for light rain and snow detection relative to TRMM*
- *Better measurement accuracy with differential attenuation correction*
- *Detailed microphysical information (DSD mean mass diameter & particle no. density) & identification of liquid, ice, and mixed-phase regions*

Multi-Channel (10-183 GHz) GPM Microwave Imager (GMI):

- *Higher spatial resolution (IFOV: 6-26 km)*
- *Improved light rain & snow detection*
- *Improved signals of solid precipitation over land (especially over snow-covered surfaces)*
- *4-point calibration to serve as a radiometric reference for constellation radiometers*

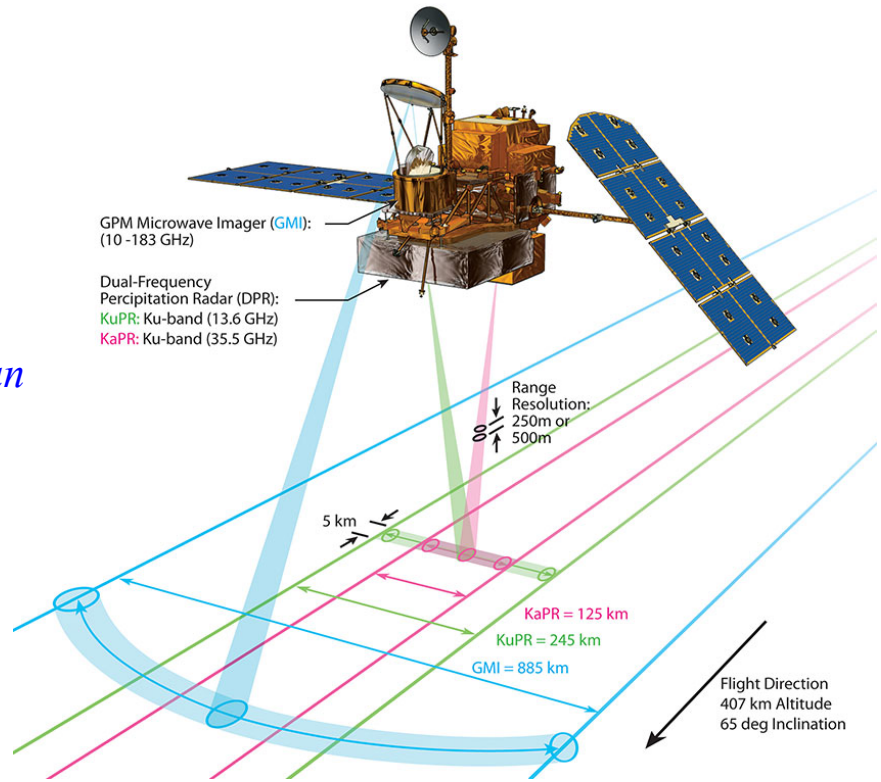

Combined Radar-Radiometer Retrieval

- *DPR & GMI together provide greater constraints on possible solutions to improve retrieval accuracy*
- *Observation-based a-priori cloud database for constellation radiometer retrievals*

Fig. from Arthur Hou